TITLE

TITOLO

PRELIMINARY DESIGN AND THERMAL-HYDRAULIC ANALYSIS OF THE HCSG FOR THE CIRCE-THETIS FACILITY

AUTHORS

AUTORI

P. Lorusso, I. Di Piazza, D. Martelli, A. Musolesi, A. Del Nevo, M. Tarantino

SUMMARY

SOMMARIO

This document reports the preliminary design of the new HCSG mock-up for the THETIS test section, providing information about the geometrical features and the instrumentation installed. A preliminary test analysis carried out by the system thermal hydraulic code RELAP5/Mod3.3 in support of the design phase is presented. The simulations performed aimed at evaluating the thermal-hydraulic performances of the component under the operative conditions foreseen during the experimental campaigns. An additional 3D CFD analysis has been carried out to assess pressure losses and flow field on the LBE shell side and to support the design of the THETIS test section.

REV.	WRITTEN/ELABORATO	CHECKED / CONVALIDA	APPROVED / APPROVAZIONE
0	Pierdomenico Lorusso	Marco Utili	Mariano Tarantino

(Page intentionally left blank)

LIST OF REVISION

Revision	Date	Scope of revision	Page
0	09/02/2021	First Issue	52

CONTENTS

LIST OF FIGURES

LIST OF TABLES

LIST OF ABBREVIATIONS

AIS	Argon Injection System
ARS	Argon Recirculation System
CIRCE	CIRcolazione Eutettico (Eutectic CIRCulation)
CFD	Computational Fluid Dynamics
ENEA	Agenzia nazionale per le nuove tecnologie, l’energia e lo sviluppo economico sostenibile
FPS	Fuel Pin Simulator
FV	Fitting Volume
GEN-IV	Generation IV
HCSG	Helical Coil Steam Generator
HERO	Heavy liquid mEtal – pRessurized water cOoled tube
LBE	Lead-Bismuth Eutectic
LFR	Lead cooled Fast Reactor
MCP	Main Circulation Pump
MYRRHA	Multi-purpose hYbrid Research Reactor for High-tech Applications
PATRICIA	Partitioning And Transmuter Research Initiative in a Collaborative Innovation Action
PHTS	Primary Heat Transfer System
RVACS	Reactor Vessel Auxiliary Cooling System
TC	ThermoCouple
THETIS	Thermal-hydraulic HElical Tubes Innovative System
TS	Test Section

(Page intentionally left blank)

1 INTRODUCTION

In the framework of the LFRs GEN-IV nuclear plants and fusion technology development, a new steam generator consisting of a helical tube bundle is currently under study. In particular, the PATRICIA (Partitioning And Transmuter Research Initiative in a Collaborative Innovation Action) project (EC – H2020) has been launched by the European Commission to support innovative solutions for the development of MYRRHA (Multi-purpose hYbrid Research Reactor for High-tech Applications), while in fusion field, EUROfusion has dedicated a task for the study of Helical Coil Steam Generators (HCSGs) to be used for the Primary Heat Transfer System (PHTS) of the DEMO plant.

In this framework, the ENEA Brasimone Research Centre supports such R&D activities through experimental campaigns, involving CIRCE (CIRColazione Eutettico), a large scale pool-type facility using Lead-Bismuth Eutectic (LBE) as the primary coolant and pressurized water as the secondary fluid. A new Test Section (TS) named THETIS (Thermal-hydraulic HElical Tubes Innovative System) for the CIRCE facility is currently under development and it will replace the HERO (Heavy liquid mEtal – pRessurized water cOoled tube) test section, which is presently installed in the CIRCE main vessel. The new test section will be characterized by new features and some new components with respect to the previous one. In particular, a vertical mechanical pump and a new prototypical HCSG will be installed and tested.

The tests foreseen for the experimental campaigns aim at investigating the thermal-hydraulic behaviour of the system in the steady state operation (forced circulation regime), during operational and accidental transients (postulated scenarios) and in natural circulation regime, as well as to characterize from a thermal-hydraulic point of view the performances of the HCSG. The stability of the system in natural circulation regime will be studied considering as heat sink the HCSG (acting as decay heat removal system) and the RVACS (Reactor Vessel Auxiliary Cooling System), in stand-alone or coupled operation.

This document reports the preliminary design of the new HCSG mock-up for the THETIS test section, providing information about the geometrical features and the instrumentation installed. A preliminary test analysis carried out by the system thermal hydraulic code RELAP5/Mod3.3 in support of the design phase is presented. The simulations performed aimed at evaluating the thermal-hydraulic performances of the component under the operative conditions foreseen during the experimental campaigns. An additional 3D CFD analysis has been carried out to assess pressure losses and flow field on the LBE shell side and to support the design of the THETIS TS.

(Page intentionally left blank)

2 CIRCE GENERAL LAYOUT

The LBE pool CIRCE is an integral effect type facility [1]. The main systems and components are:

- S100 main vessel, conceived to host the test sections. It has an inner diameter of 1170 mm, a thickness of 15 mm, and a height of about 8500 mm. It is partially filled with about 70 tons of LBE and argon as cover gas maintained in slight overpressure. The main vessel is insulated by rock wool to minimize the thermal losses in the environment and it is equipped with electrical heating cables, installed on its bottom and lateral surfaces. The heating cables can reach an operating temperature range of 250÷300°C. The cover gas of the main vessel is also equipped by a self-controlled discharge system and a passive pressure safety system (rupture disks), in order to prevent accidental overpressure;
- S200 storage tank, in which the LBE is stored during the periods of maintenance and refurbishment of the facility;
- S300 transfer tank, used during the filling and draining phases of the main vessel;
- the Argon Recirculation System (ARS): the ARS is equipped by a set of 5 compressors connected in parallel and an argon storage tank, acting as gas lung and directly connected to external gas tanks used for argon re-integration;
- RVACS, which allows the cooling of the external surface of the vessel by mean of air injection;
- a once-through secondary loop to supply water to the HCSG at a maximum pressure of ~18 MPa and a temperature of 335°C.

A new test section (Fig. 1) is currently under development and it will be composed of the following components:

- Fuel Pin Simulator (FPS), electrically heated for the coolant heating; it consists of an electrical pin bundle composed by 37 electrically heated pins with a nominal thermal power of 925 kW; the FPS is already installed in the facility and it is instrumented;
- Fitting Volume (FV) which collects the hot LBE rising from the FPS;
- riser connecting the FV to the pump suction;
- Main Circulation Pump (MCP) to perform LBE forced circulation [2];
- hot pool (separator) which will feed the HCSG;
- HCSG for the heat removal from the primary system; this component works in counter-flow, with the LBE flowing shell side downwards and the water flowing tube side;
- dead volume, which encloses and maintains insulated the power supply rods feeding the FPS.

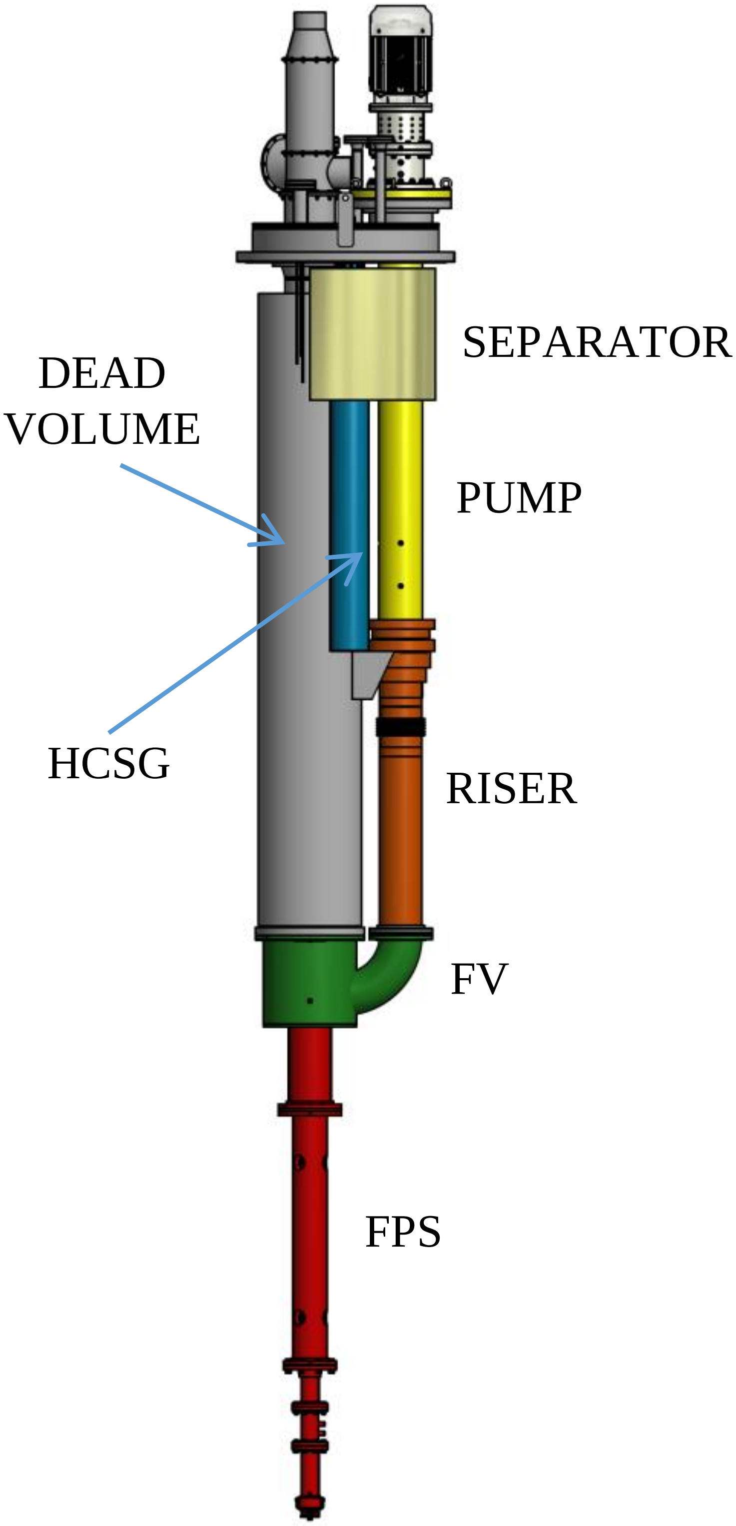

Fig. 1 – Schematic view of the THETIS Test Section

3 PRELIMINARY REQUIREMENTS

The preliminary analysis to assess the main operative parameters of the facility has been performed in detail in [3]. The reference thermal cycle to be performed in the primary side foresees the achievement of a temperature inlet-outlet of the LBE in the HCSG shell side of 480-400°C. Assuming as a conservative assumption (observed from previous experience [4][5]) the presence of heat losses along the LBE flow path between FPS and steam generator, it can be considered in first approximation a temperature difference inlet-outlet along the FPS of 400-490°C.

For a first calculation, the value of thermal power removed by the HCSG has been assumed to be 400kW, thus the power to be supplied by the FPS is derived as a consequence. The power values are defined considering that the maximum electrical power available for the heating of LBE and water is 1.2 MW and that, during the previous experiments, the power needed by the primary side for LBE heating and by the secondary side for water pre-heating were comparable. Since the water conditions are similar for the new tests, it can be expected that also the needed power ratio between primary and secondary systems will be similar to that observed during the CIRCE-HERO experimental campaign . In this way, it is possible to conclude that, assuming 400kW as the HCSG power, a similar value can be expected for the secondary system, achieving a total power needed for the facility operation in the range of 800-900 kW, assuring a good margin respect to the maximum power of 1.2 MW available for the LBE and water heating. The operation of the ancillary systems (e.g. water pump, heating cables) is assured by an additional electrical power supply of 140 kW.

The LBE mass flow rate needed to achieve a ΔT of 80°C between the inlet and outlet of the HCSG can be calculated applying the thermal balance equation (Eq. 1):

$$\dot{m}_{LBE} = \frac{P_{w,HCSG}}{C_{p,LBE}(T_{LBE-i} - T_{lbe-o})} \qquad \text{Eq 1}$$

where:

- $P_{w,HCSG}$ is the thermal power removed by the HCSG expressed in W;
- T_{LBE-i} / T_{LBE-o} are the inlet and outlet temperatures in the HCSG;
- $\dot{m}$ is the mass flow rate
- c_p is the LBE isobaric specific heat (J/kg*K) evaluated by the following correlation [6] (temperature is expressed in Kelvin):

$$c_{p,LBE} = 164.8 - 3.94 * 10^{-2}T + 1.25 * 10^{-5}T^2 - 4.56 * 10^5T^{-2} \qquad \text{Eq 2}$$

obtaining a value of 142.1 J/(kg*K), assuming an average LBE temperature of 440°C.

With these conditions, the LBE mass flow rate needed for the achievement of the steady state condition is 35.2 kg/s .

It is possible to evaluate the power to be supplied by the FPS to achieve the temperature of 490°C at the outlet section of the pin bundle. Assuming a temperature difference of 90°C, the LBE mass flow rate of 35.2 kg/s and the isobaric specific heat from Eq.2, the FPS power can be calculated using the Eq.1, obtaining in such a way a power value of 450 kW.

Furthermore, other LBE thermal cycles with different temperature ranges are also considered, assuming constant the power removed by the HCSG. In particular, the temperature differences of 60°C (480-420°C) and 40°C (480-440°C) along the shell side of the HCSG are also considered. Using the Eq. 1 and Eq. 2 it is possible to calculate the FPS power range which is in the range of 450-500 kW. The results of the calculation are summarized in Tab. 1.

Parameter	Case1	Case2	Case3
SG T inlet-outlet [°C]	480-400	480-420	480-440
FPS T inlet-outlet [°C]	400-490	420-490	440-490
ΔT HCSG [°C]	80	60	40
ΔT FPS [°C]	90	70	50
T_{avg} HCSG [°C]	440	450	460
T_{avg} FPS [°C]	445	455	465
Cp LBE [J/kg*k]	142.1	142	141.8
Power HCSG [kW]	400	400	400
Power FPS [kW]	450	467	500
LBE mass flow rate [kg/s]	35.17	46.96	70.53

Tab. 1 – Primary side thermal cycles

On the secondary side, an operating pressure range between 9-18 MPa is foreseen. In particular, the tests at 18 MPa will be performed in support of fission applications (i.e. PATRICIA project), while the tests with pressure range 9-12 MPa will be executed in support of fusion applications (i.e. EUROfusion WPBoP). In the following, three cases at 9 MPa, 12 MPa and 18 MPa will be analyzed for each primary side conditions (i.e. LBE mass flow rate). The results of the preliminary calculation are summarized in Tab. 2.

Assuming for all the three cases few degrees of sub-cooling at the HCSG inlet, the water inlet temperature has been set at 300°C for the case at 9 MPa ($T_{sat,9MPa}$ = 303.35 °C), 320°C for the case at 12 MPa ($T_{sat,12MPa}$ = 324.68 °C) and 335°C for the case at 18 MPa ($T_{sat,18MPa}$ = 356.99 °C). A higher degree of sub-cooling for the case at 9 MPa and 12 MPa will be considered during the HCSG operation, if necessary. During the normal operation, the HCSG will be designed to produce steam with a good degree of superheating. For this reason, a preliminary value of 400°C has been considered for the steam outlet temperature.

The feedwater mass flow rate needed to remove the thermal power of 400 kW, with the outlet steam conditions specified above, can be calculated as follows:

$$\dot{m}_{H2O} = \frac{P_w}{\Delta h_{sub-cooling} + \Delta h_{vap} + \Delta h_{superheating}} \qquad \text{Eq 3}$$

where:

- P_w is the thermal power removed by the HCSG;
- $\Delta h_{sub-cooling}$ is the enthalpy needed to warm-up the water from the inlet temperature up to the saturation temperature at the reference pressure;
- Δh_{vap} is the enthalpy needed to the complete vaporization of the water at the reference pressure;
- $\Delta h_{superheating}$ is the enthalpy needed to produce superheated steam at the reference pressure.

Using the water thermal properties reported in [7], the liquid water enthalpy and steam enthalpy can be derived for each thermal cycle, obtaining in this way the feedwater mass flow rate to be supplied to the HCSG for the three cases (see Tab. 2).

A further preliminary calculation can be performed to evaluate the power needed by the helical pre-heater to warm up the feedwater from the environment temperature up to the HCSG inlet temperature. The following equation can be used:

$$P_w = \dot{m}_{H2O} * (h_{out} - h_{in}) \qquad \text{Eq 4}$$

- P_w is the thermal power supplied by the pre-heater;
- h_{in} is the water enthalpy at the inlet section of the pre-heater;
- h_{out} is the water enthalpy at the outlet section of the pre-heater.

Assuming a pre-heater inlet temperature of 10°C, a pre-heater outer temperature equal to 300°C (case at 9 MPa), 320 °C (case at 12 MPa) and 335°C (case at 18 MPa) and the mass flow rates calculated above, it is possible to obtain the pre-heating thermal power needed for the three cases (see Tab. 2).

Assuming an FPS power of 500 kW and a MCP power of 15 kW, the total power needed for the facility operation is ~806.58 kW for the cycle at 9 MPa, ~868.5 kW for the case at 12 MPa and ~957.1 kW for the case at 18 MPa. It can be concluded that in all the three cases the total power is below the maximum power of 1.2 MW available for LBE and water heating, thus, in general, **the power to be removed by the HCSG has to be within the maximum range of 400-450 kW in order to respect the maximum power available of 1.2 MW**.

Parameter	Thermal cycle 9 MPa	Thermal cycle 12 MPa	Thermal cycle 18 MPa
T sat [°C]	303.35	324.68	356.99
T inlet [°C]	300	320	335
Sub-cooling [°C]	3.35	4.68	21.99
T outlet steam [°C]	400	400	400
Δh vap [kJ/kg]	1379.20	1194.30	777.51
Δh superheating [kJ/kg]	375.87	366.31	376.78
Δh liquid-sat [kJ/kg]	19.38	31.01	188.45
Δh tot [kJ/kg]	1774.45	1591.62	1342.73
Power [kW]*	400	400	400
H2O mass flow rate [kg/s]	**0.23**	**0.25**	**0.3**
T inlet heater [°C]	10	10	10
Δh pre-heating [kJ/kg]**	1293.52	1406.67	1484.18
Power pre-heating [kJ/kg]* **	**291.6**	**353.5**	**442.1**

**neglecting the heat losses through the loop*
***at 95 bar and 125 bar, considering the pressure drop of the loop*
****neglecting the heat losses from the pre-heater and the efficiency of the component*

Tab. 2 – Secondary loop main requirements

4 HCSG LAYOUT

The steam generator for the THETIS TS consists of a prototypical solution with a helical tube bundle, which assures a high power removed, taking up the minimum amount of space. The HCSG is conceived to work in counter flow, with LBE as the primary coolant, flowing along the shell side, and pressurized water as the secondary coolant, flowing in the tube side. This section reports the HCSG preliminary design, presenting the final layout achieved at the end of the design optimization process performed with the system thermal-hydraulic code RELAP5/Mod3.3. From the previous experimental campaigns performed on the HERO TS [5][8], it has been observed that assuming the same LBE conditions (SG inlet temperatures and flow rates) and the same water mass flow rate, the higher performances, and thus the higher power fraction removed, have been achieved for the test at operating pressure in range of 8-12 MPa. For this reason, **in order to be conservative during the HCSG design phase, the maximum power range condition of 400-450 kW has been applied for the case at 9 MPa for the reference conditions ($T_{LBE,in}/T_{LBE,out}$ = 480°C/400°C, LBE mass flow rate 35.2 kg/s).**

The 2D and 3D views of the component are depicted in Fig. 2 and Fig. 3. The technical drawing is reported in APPENDIX 1. The preliminary layout of the HCSG is composed of:

- a top flange (ex-vessel) with a perforated plate to accommodate the downcomer tubes (15 holes) and the riser tubes. The flange connects the HCSG to the CIRCE main vessel and it sustains the feedwater manifold, the steam chamber, the tube bundle and the inner shell;
- a feedwater manifold (ex-vessel) for the feedwater distribution among the tubes. The manifold is welded above the top flange and it has appropriate holes to accommodate the riser tubes which are fixed to the holes by welding to avoid leakages;
- a straight tube dowcomer bundle, having 15 tubes 3/8” BWB 16 and a height of 1.5 m, which feeds the helical tube rising bundle;
- a helical tube rising bundle (in-vessel), with 15 tubes 3/8” BWB 16, having a height of 1.5 m, in which the vaporization occurs;
- a steam chamber in which the steam produced is collected (ex-vessel), connected to the discharge line;
- an inner double wall shell, having a height of 1.5 m from the separator bottom, in which the straight tube downcomer bundle is enclosed (in-vessel). The shell is composed of two coaxial shells forming a gap filled by air acting as an insulator between the LBE inside the inner shell and the LBE flowing in the annular region between the inner and outer shells;
- an outer double wall shell, having a height of 1.62 m from the separator bottom, surrounding the helical tube riser bundle (in-vessel). The shell is composed by two coaxial shells forming a gap filled by air acting as insulator between the LBE flowing in the annular region between the inner and outer shells and the LBE inside the S100;
- dedicated spacers will be foreseen in order to keep the tubes in position.

Each tube starts from the feedwater manifold on the top part of the HCSG and it goes down straight up to the bottom part, where it curves and rises with a helical shape up to the steam chamber. The coil inclination angle and the vertical pitch are managed in order to maintain constant the length of each helix. The horizontal pitch of the helical ranks is designed to avoid bypass zones for the LBE flow.

The helical tubes are arranged in three horizontal ranks: the inner rank is composed of 4 tubes, the intermediate one is composed of 5 tubes and the outer rank has 6 tubes. The minimum horizontal rank number of 3 is required, in order to assure the representativeness of the component respect to the systems of interest and to reproduce in a reliable way the main phenomena involved.

The three horizontal ranks are wrapped in alternate directions: the inner and outer rank have a clockwise direction, while the intermediate rank has a counterclockwise direction. This configuration aims at reducing the LBE secondary circulation due to the helical shape. This aspect has been investigated in a dedicated CFD analysis reported in the next paragraphs. Actually, a strong secondary circulation takes place in the LBE shell side.

The design of the helical tube bundle has been performed setting at first the tube size, the linear height (H), the vertical ranks pitch (P_{vr}) and the horizontal ranks pitch (P_{hr}). In such a way, the vertical and horizontal pitch/diameter ratios are defined. Then, the number of tubes is calculated imposing a feedwater velocity and the total number of tubes is divided among the ranks in order to maintain constant the length of each helix. The coil vertical pitch (P_c) for each rank can be defined as the ratio between the vertical rank pitch and the number of tubes of the corresponding rank. The radius of the coils (R_c) is assumed on the basis of the size of the double wall inner shell. The inclination of the tubes (α) and the length of each helix (L_h) can be calculated by the following equations:

$$\alpha = arctg\left(\frac{P_c}{2\pi R_c}\right) \qquad \text{Eq 5}$$

$$L_h = \left(\frac{H}{P_c}\right) * \sqrt{(2\pi R_c)^2 + (P_c)^2} \qquad \text{Eq 6}$$

The geometrical features of the helical bundle are introduced in the RELAP5 model and a first run is launched. From the outcomes of the simulation, it is possible to evaluate the performances of the bundle and to modify the geometrical parameters introduced above, if necessary. The changes in geometry are included in the RELAP5 input deck and a new run is launched. This iterative calculation is performed until the required operating conditions are met.

The helical tube bundle is enclosed between a double wall outer shell and a double wall inner shell, as shown in Fig. 4. During the operation, the total LBE mass flow rate passes through the annular region formed between the two shells, allowing the heat exchange with the helical tube bundle only. The downcomer bundle is enclosed in a double wall inner shell (see Fig. 4), where the LBE is stagnant. This implies that the heat exchange between the descending feedwater and the stagnant

LBE is strongly reduced since during the operation the two coolants reach almost the same temperature. In this way, the vaporization occurs in the ascending helical tubes only, avoiding eventual flow instabilities in the tubes during the HCSG operation.

The gap within the double wall of the two shells is filled by air acting as a thermal insulator. This allows to avoid the heat exchange from the hot LBE flowing in the annular region to the stagnant LBE inside the inner shell and the LBE in the main pool, enhancing in such a way the thermal-hydraulic performances of the component.

Details on the geometrical data of the HCSG are reported in Tab. 2 and Tab. 3.

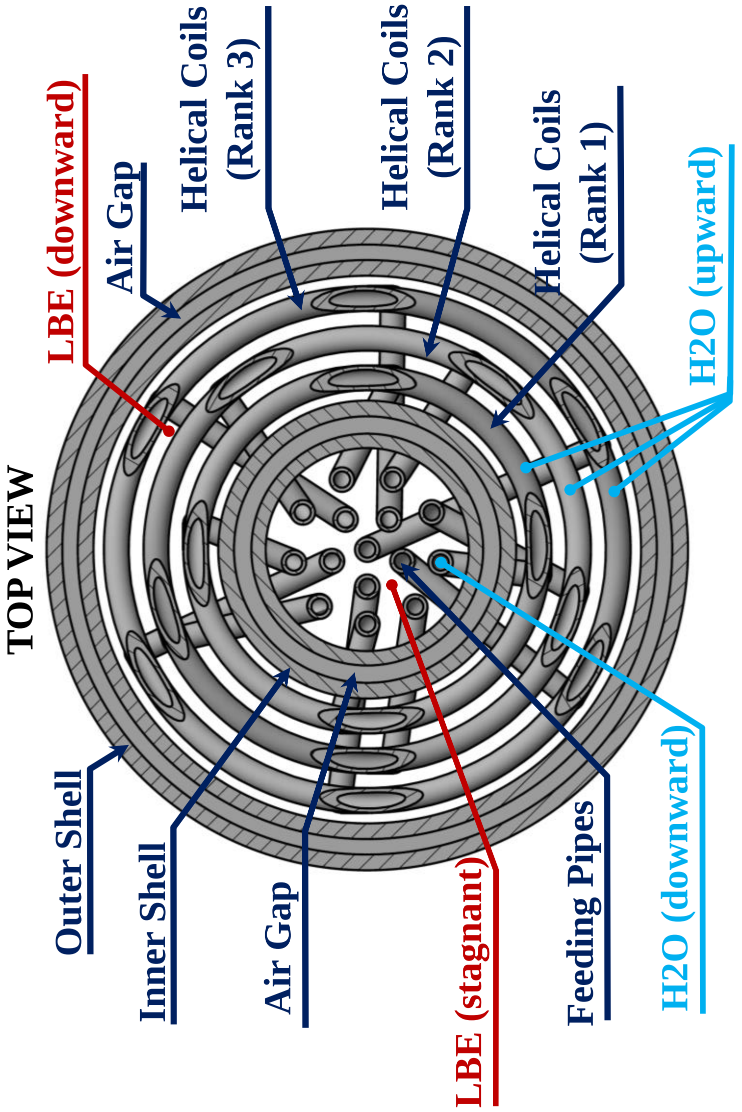

Fig. 2 – Top view of the HCSG

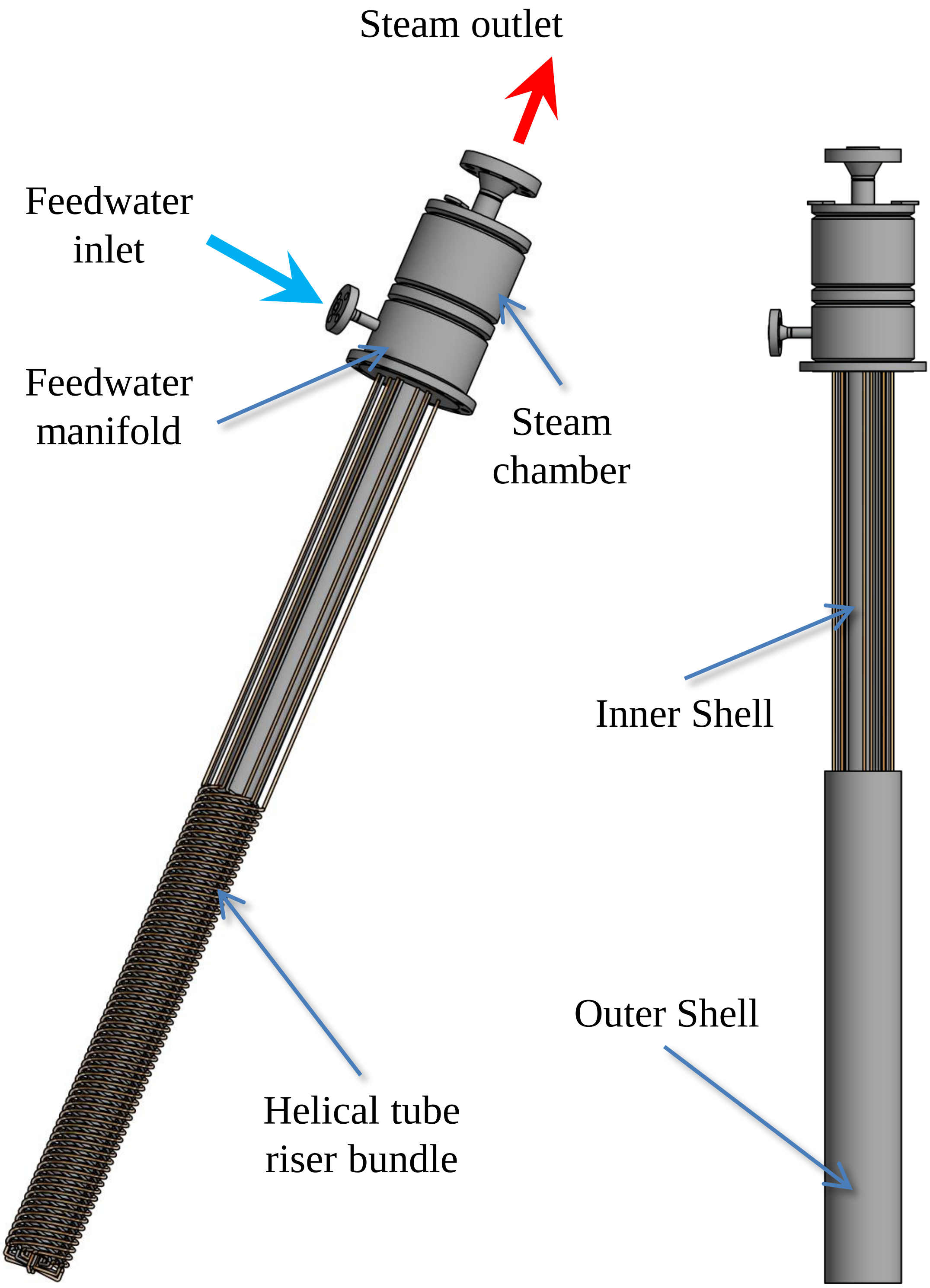

Fig. 3 – 3D view of the HCSG

Geometrical Data	Unit	Horizontal Rank N°1 (inner)	Horizontal Rank N°2 (middle)	Horizontal Rank N°3 (outer)
Height	[m]	1.5	1.5	1.5
Tubes I.D.	[m]	0.00622	0.00622	0.00622
Tubes O.D.	[m]	0.00952	0.00952	0.00952
N° of tubes (vertical ranks)	----	4	5	6
Horizontal P/D	----	1.6	1.6	1.6
Horizontal Pitch	[m]	0.0152	0.0152	0.0152
D helix*	[m]	0.132	0.162	0.193
Coil Vertical P/D	----	10.08	12.61	15.13
Coil Vertical Pitch	[m]	0.096	0.120	0.144
Inclination angle	----	13.05°	13.24°	13.38°
L coil (active length)	[m]	6.642	6.547	6.484
Total length 1 tube*	[m]	8.142	8.047	7.984
Vertical Pitch	[m]	0.024	0.024	0.024
Vertical P/D	----	2.521	2.521	2.521
L tot (active length)***	[m]	26.569	32.735	38.901

**Considering the tube axis*
***(L coil + 1.5 m) – lower and upper connections not included*
****lower connections not included*

Tab. 3 – Main geometrical parameters of the HCSG tube bundle

Geometrical Data	Unit	I..D.	Thickness	O.D.
Inner Shell (H=1.5 m)				
Inner Tube	[m]	0.07792	0.00549	0.0889
Air Gap	[m]	0.0889	0.00668	0.10226
Outer Tube	[m]	0.10226	0.00602	0.1143
Outer Shell (H=1.62 m)				
Inner Tube	[m]	0.21027	0.006	0.22227
Air Gap	[m]	0.22227	0.006	0.23427
Outer Tube	[m]	0.23427	0.006	0.24627

Tab. 4– Main geometrical data of the HCSG shells

5 HCSG INSTRUMENTATION

An overall number of 41 TCs (hot junction isolated, *N*-type) is implemented in the LBE side of the HCSG at the following positions [9]:

- ***3 TCs*** are positioned at 120° at the inlet section of the SG (**TC-SG-01**, **TC-SG-02**, **TC-SG-03**, 3 mm diameter) to measure the LBE inlet temperature;
- ***3 TCs*** are installed at 120° at the outlet section (**TC-SG-04**, **TC-SG-05**, **TC-SG-06**, 3 mm diameter) to measure the LBE outlet section;
- ***30 TCs*** having a diameter of 1 mm are positioned at four different sections to monitor the LBE (15 TCs) and wall (15 TCs) temperatures. The TCs are arranged in order to have two TCs installed on each tube, which acts as a support for the TCs up to the measure points. The sections are fixed at four different levels, assuming as level 0.0 mm the bottom part of the helical tubes, as detailed in Fig. 6. ***2 additional TCs*** are added in two specific sections and supported by the SG outer shell. The distribution of the TCs is performed as follows:

  - *Level 1* (+300 mm), 7 TCs (4 bulk, 3 wall) are installed to monitor all the sub-channels identified by the tube horizontal ranks and the inner and outer shells walls. The TCs are positioned in such a way to have bulk and tube wall temperature measurements along the same radial direction. Details on the TCs position are reported in Tab. 6 and Fig. 7;
  - *Level 2* (+600 mm), 8 TCs (4 bulk, 4 wall) are installed for temperature measurements in all the sub-channels. The TCs are positioned in such a way to have bulk and tube wall temperature measurement along the same radial direction, excepting for the outer sub-channel (between the inner wall of the outer shell and the outer tube rank). Details on the TCs position are reported in Tab. 7 and Fig. 8;
  - *Level 3* (+900 mm), 10 TCs (5 bulk, 5 wall) are installed to monitor all the sub-channels at different positions in the same section. Details on the TCs position are reported in Tab. 8 and Fig. 9;
  - *Level 4* (+1200 mm), 7 TCs (4 bulk, 3 wall) are installed to monitor all the sub-channels. The TCs are positioned in such a way to have bulk and tube wall temperature measurement along the same radial direction. Details on the TCs position are reported in Tab. 9 and Fig. 10.

- ***3 TCs*** (**TC-SG-07**, **TC-SG-08**, **TC-SG-09**, 3 mm diameter) are installed inside the HCSG stagnant volume to monitor the temperature of the stagnant LBE. In particular, the TCs are positioned at 3 different levels: Level 1 (300 mm from the SG bottom), Level 3 (900 mm) and SG inlet section. The TCs are listed in Tab. 10 and reported in Fig. 11.

On the secondary side, the water temperature will be monitored at the HCSG inlet section (2 TCs upstream the feedwater manifold) and outlet section (3 TCs downstream the steam chamber). In particular, three TCs are set at the outlet section of the steam chamber, for temperature monitoring in the bottom (condensation feedback), center and higher part (stratification evaluation) of the flow section (Tab. 11). The overall pressure drops across the feedwater manifold and steam chamber is acquired by a differential pressure transmitter (Tab. 11).

The LBE mass flow rate is computed on the basis of **DP-Ven** signal (**Mm(LBE)**) of the Venturi Flow Meter installed upstream the FPS and of power and temperature increase through the FPS, **Mm(LBE,HS)**. Furthermore, derived quantities are the power removed from the LBE and acquired by water through HCSG (**Q-SG-LBE** and **Q-SG-H_2O**, respectively).

N°	ID	Description	Measurement position	Diam. [mm]	Ref.	Notes
1	**TC-SG-01**	LBE inlet temperature	HCSG inlet section (θ= 0°)	1	Fig. 4	
2	**TC-SG-02**	LBE inlet temperature	HCSG inlet section (θ= 120°)	"	Fig. 4	
3	**TC-SG-03**	LBE inlet temperature	HCSG inlet section (θ= 240°)	"	Fig. 4	
4	**TC-SG-04**	LBE outlet temperature	HCSG outlet section (θ= 0°)	"	Fig. 4	
5	**TC-SG-05**	LBE outlet temperature	HCSG outlet section (θ= 120°)	"	Fig. 4	
6	**TC-SG-06**	LBE outlet temperature	HCSG outlet section (θ= 240°)	"	Fig. 4	

Tab. 5 – HCSG LBE side – TCs positions at the inlet and outlet section

N°	ID	Description	Measurement position	Diam. [mm]	Ref.	Notes
1	**TC-B12-L1**	LBE temperature	Rank 1, Tube 2, Level 1	3	Fig. 7	
2	**TC-W12-L1**	Wall temperature	Rank 1, Tube 2, Level 1 (wall embedded)	"	Fig. 7	
3	**TC-B23-L1**	LBE temperature	Rank 2, Tube 3, Level 1	"	Fig. 7	
4	**TC-W23-L1**	Wall temperature	Rank 2, Tube 3, Level 1 (wall embedded)	"	Fig. 7	
5	**TC-B32-L1**	LBE temperature	Rank 3, Tube 2, Level 1	"	Fig. 7	
6	**TC-W32-L1**	Wall temperature	Rank 3, Tube 2, Level 1 (wall embedded)		Fig. 7	
7	**TC-BS1-L1**	LBE temperature	External channel, Level 1		Fig. 7	

Tab. 6 – HCSG LBE side – TCs positions at Level 1 (+300 mm)

N°	ID	Description	Measurement position	Diam. [mm]	Ref.	Notes
1	**TC-B11-L2**	LBE temperature	Rank 1, Tube 1, Level 2	"	Fig. 8	
2	**TC-W11-L2**	Wall temperature	Rank 1, Tube 1, Level 2 (wall embedded)	"	Fig. 8	
3	**TC-B22-L2**	LBE temperature	Rank 2, Tube 2, Level 2	"	Fig. 8	
4	**TC-W22-L2**	Wall temperature	Rank 2, Tube 2, Level 2 (wall embedded)	"	Fig. 8	
5	**TC-B31-L2**	LBE temperature	Rank 2, Tube 1, Level 2	"	Fig. 8	
6	**TC-W31-L2**	Wall temperature	Rank 2, Tube 1, Level 2 (wall embedded)	"	Fig. 8	
7	**TC-B36-L2**	LBE temperature	Rank 3, Tube 6, Level 2	"	Fig. 8	
8	**TC-B36-L2**	Wall temperature	Rank 3, Tube 6, Level 2 (wall embedded)	"	Fig. 8	

Tab. 7 – HCSG LBE side – TCs positions at Level 2 (+600 mm)

N°	ID	Description	Measurement position	Diam. [mm]	Ref.	Notes
1	**TC-B13-L3**	LBE temperature	Rank 1, Tube 3, Level 3	"	Fig. 9	
2	**TC-W13-L3**	Wall temperature	Rank 1, Tube 3, Level 3 (wall embedded)	"	Fig. 9	
3	**TC-B24-L3**	LBE temperature	Rank 2, Tube 4, Level 3	"	Fig. 9	
4	**TC-W24-L3**	Wall temperature	Rank 2, Tube 4, Level 3 (wall embedded)	"	Fig. 9	
5	**TC-B21-L3**	LBE temperature	Rank 2, Tube 1, Level 3	"	Fig. 9	
6	**TC-W21-L3**	Wall temperature	Rank 2, Tube 1, Level 3 (wall embedded)	"	Fig. 9	
7	**TC-B33-L3**	LBE temperature	Rank 3, Tube 3, Level 3	"	Fig. 9	
8	**TC-B33-L3**	Wall temperature	Rank 3, Tube 3, Level 3 (wall embedded)	"	Fig. 9	
9	**TC-B35-L3**	LBE temperature	Rank 3, Tube 5, Level 3		Fig. 9	
10	**TC-W35-L3**	Wall temperature	Rank 3, Tube 5, Level 3 (wall embedded)		Fig. 9	

Tab. 8 – HCSG LBE side – TCs positions at Level 3 (+900 mm)

N°	ID	Description	Measurement position	Diam. [mm]	Ref.	Notes
1	**TC-B14-L4**	LBE temperature	Rank 1, Tube 4, Level 4	"	Fig. 10	
2	**TC-W14-L4**	Wall temperature	Rank 1, Tube 4, Level 4 (wall embedded)	"	Fig. 10	
3	**TC-B25-L4**	LBE temperature	Rank 2, Tube 5, Level 4	"	Fig. 10	
4	**TC-W25-L4**	Wall temperature	Rank 2, Tube 5, Level 4 (wall embedded)	"	Fig. 10	
5	**TC-B34-L4**	LBE temperature	Rank 3, Tube 4, Level 4	"	Fig. 10	
6	**TC-W34-L4**	Wall temperature	Rank 3, Tube 4, Level 4 (wall embedded)	"	Fig. 10	
7	**TC-BS4-L4**	LBE temperature	External channel, Level 4	"	Fig. 10	

Tab. 9 – HCSG LBE side – TCs positions at Level 4 (+1200 mm)

N°	ID	Description	Measurement position	Diam. [mm]	Ref.	Notes
1	**TC-SG-07**	LBE temperature	Inside the dead volume at Level 1 (300 mm from the SG bottom)	3	Fig. 11	
2	**TC-SG-08**	LBE temperature	Inside the dead volume at Level 3 (900 mm from the SG bottom)	"	Fig. 11	
3	**TC-SG-09**	LBE temperature	Inside the dead volume at SG inlet (1500 mm from the SG bottom)	"	Fig. 11	

Tab. 10 – HCSG LBE side – TCs positions inside the stagnant volume

N°	ID	Description	Measurement position	Diam. [mm]	Ref.	Notes
1	**TC-FM-01**	H2O temperature	Upstream the feedwater manifold	3		
2	**TC-FM-02**	H2O temperature	Upstream the feedwater manifold	"		
3	**TC-SC-01**	H2O temperature	Downstream the steam chamber	"		
4	**TC-SC-02**	H2O temperature	Downstream the steam chamber			
5	**TC-SC-03**	H2O temperature	Downstream the steam chamber			
6	**DP-SG-01**	Differential pressure transmitter	Across the feedwater manifold and the steam chamber	----		

Tab. 11 – HCSG H2O side instrumentation

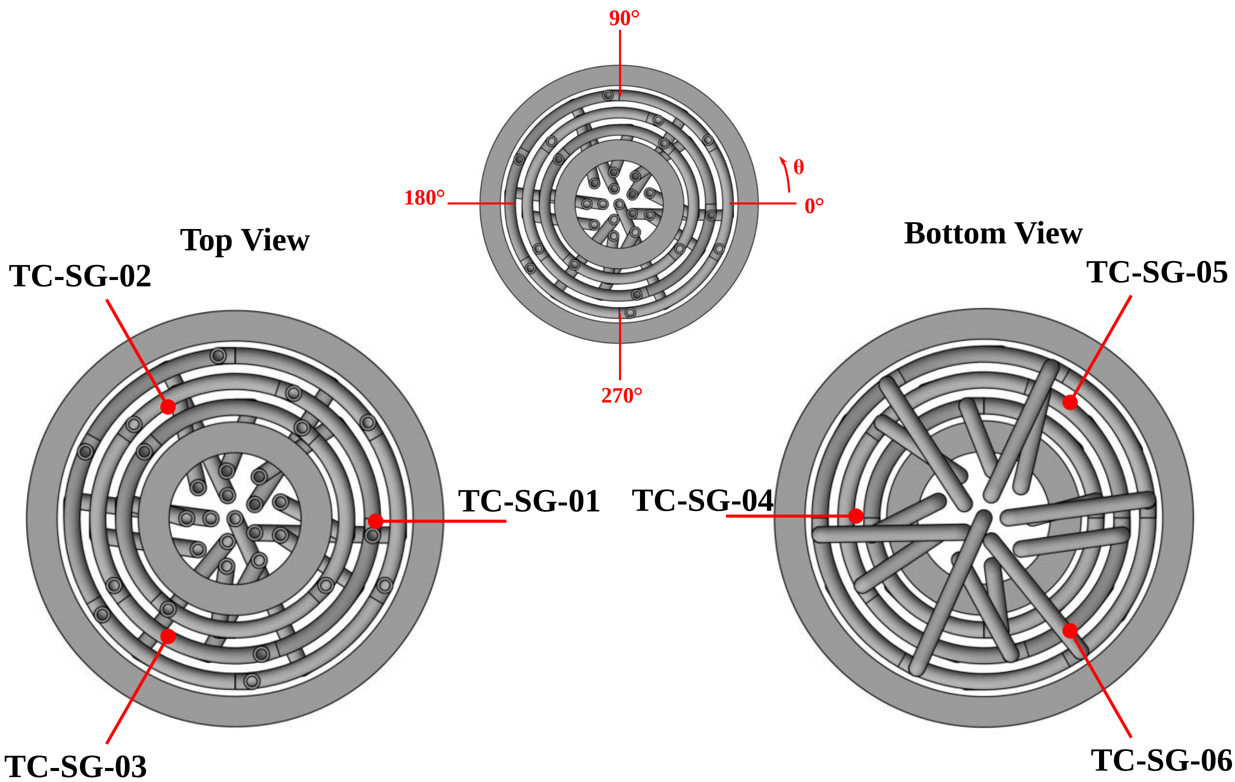

Fig. 4 – TCs at the inlet and outlet sections of the HCSG

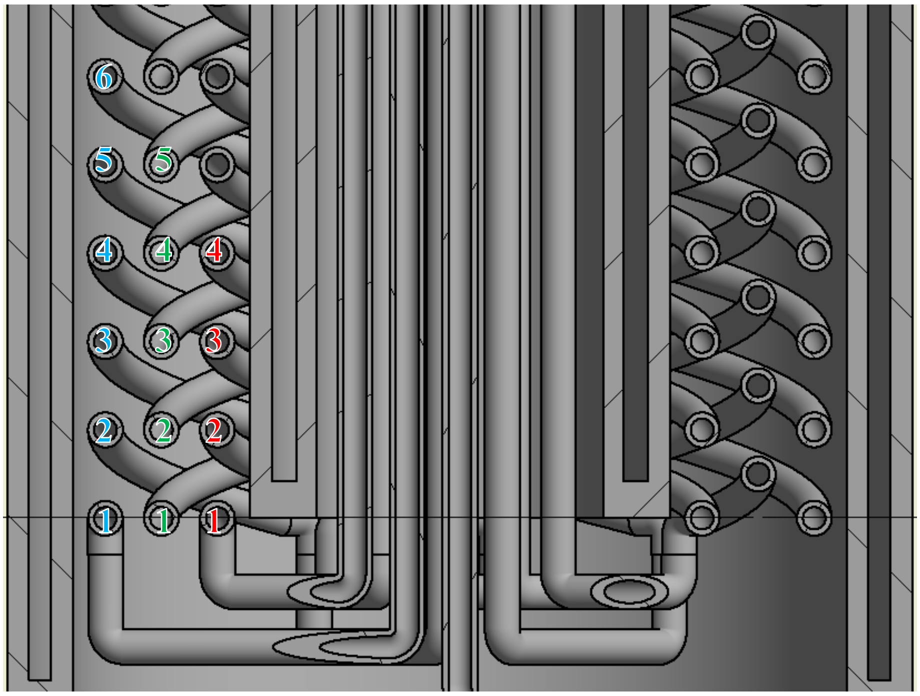

Fig. 5 – Detail of the helical tube bundle showing the ID number of each tube for each rank

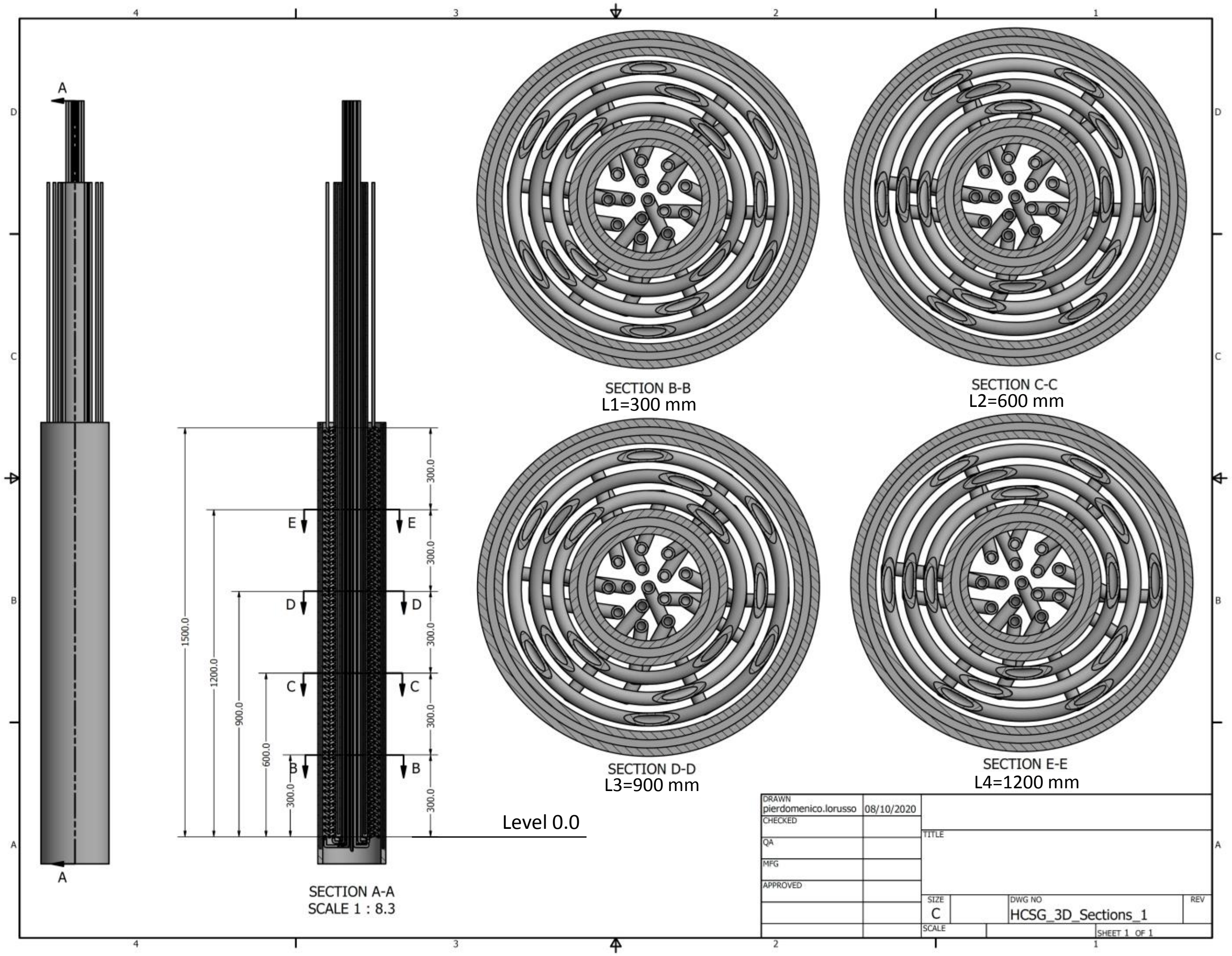

Fig. 6 – HCSG instrumentation: details of the section levels

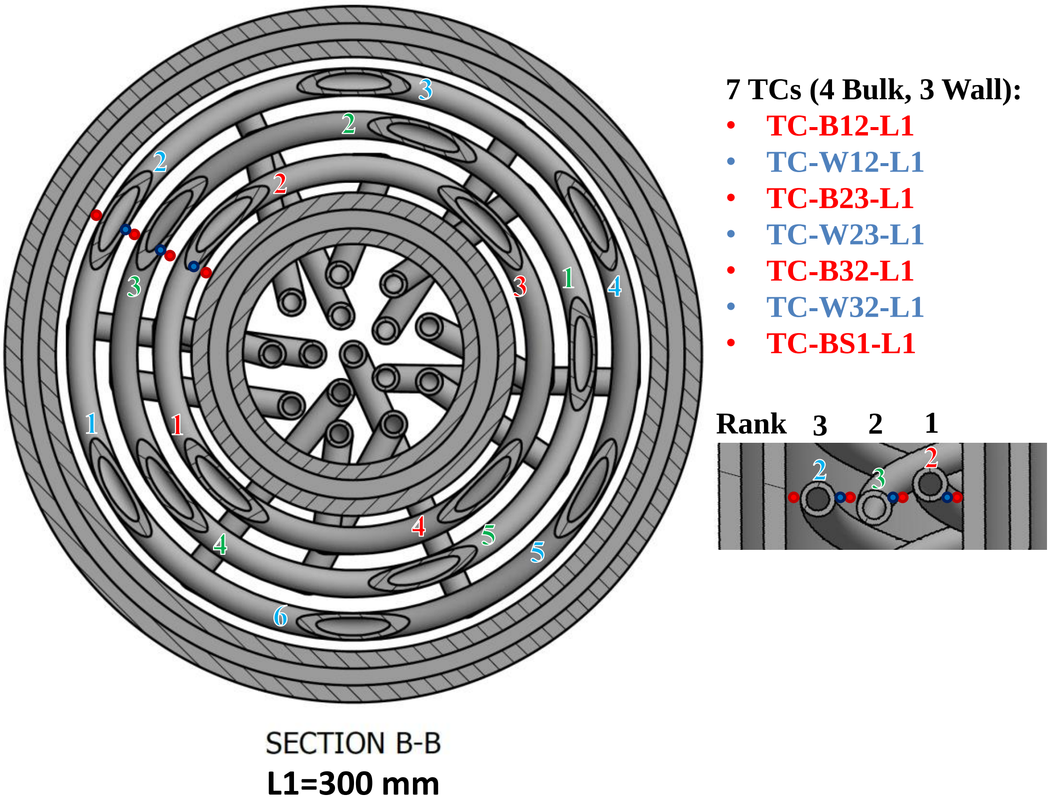

Fig. 7 – HCSG instrumentation: bulk TCs (red) and wall TCs (blue) at the Level 1

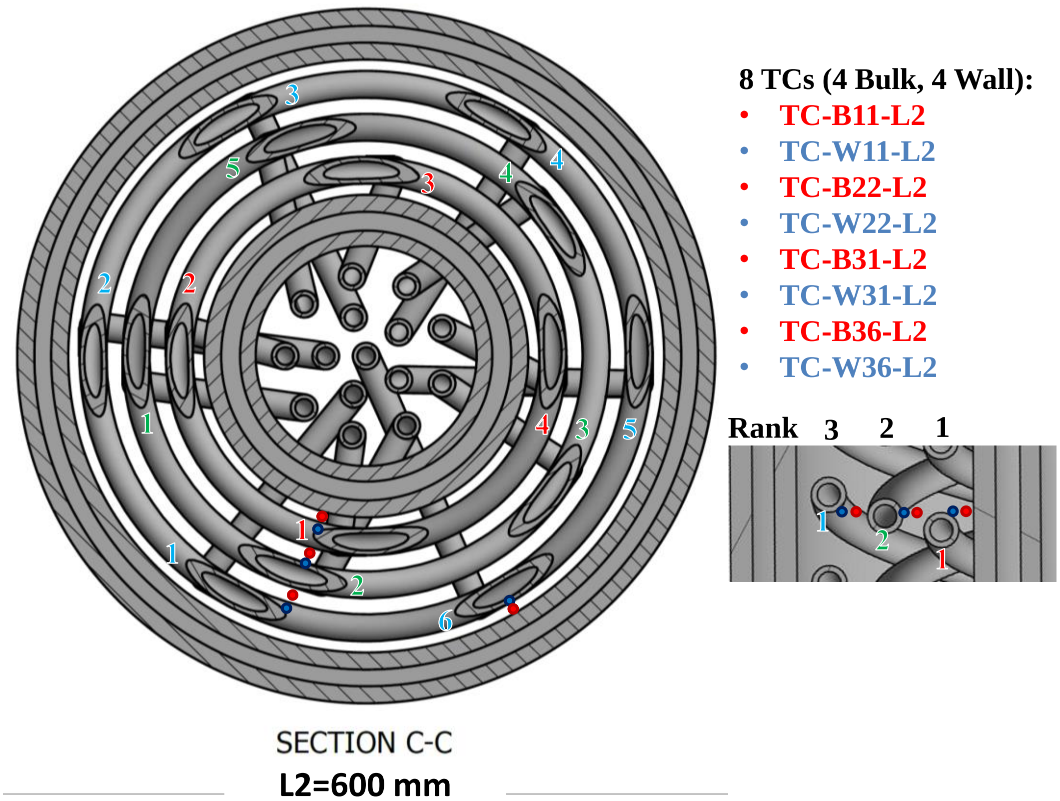

Fig. 8 – HCSG instrumentation: bulk TCs (red) and wall TCs (blue) at the Level 2

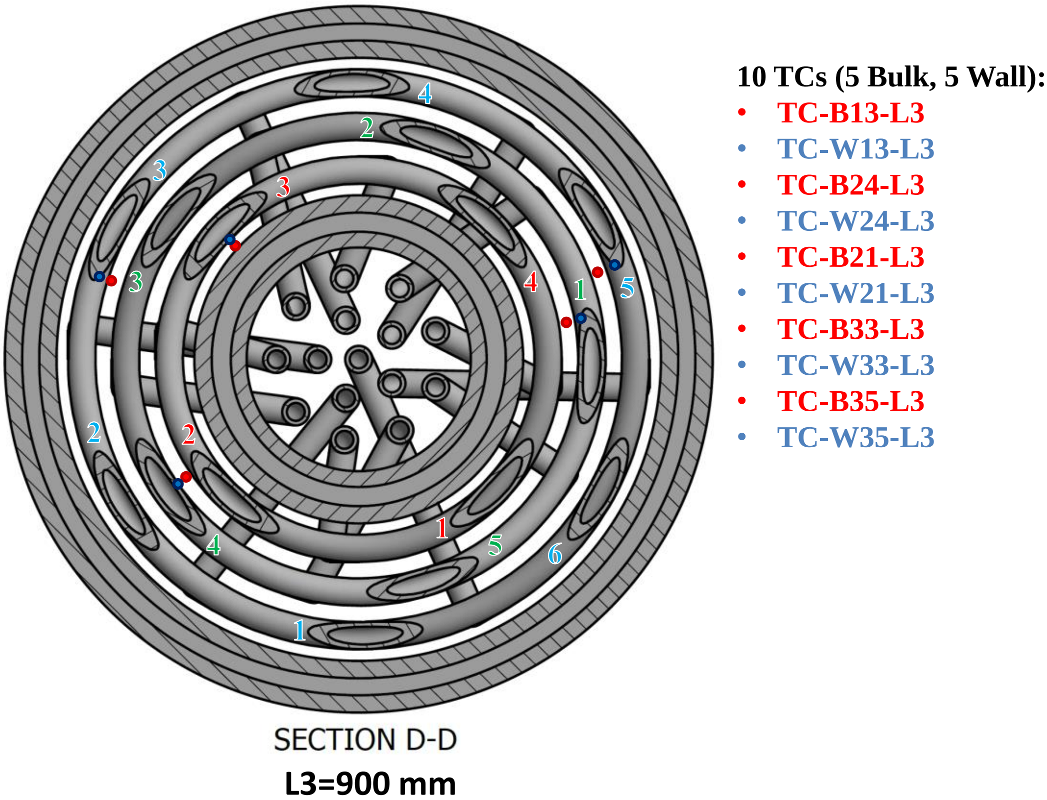

Fig. 9 – HCSG instrumentation: bulk TCs (red) and wall TCs (blue) at the Level 3

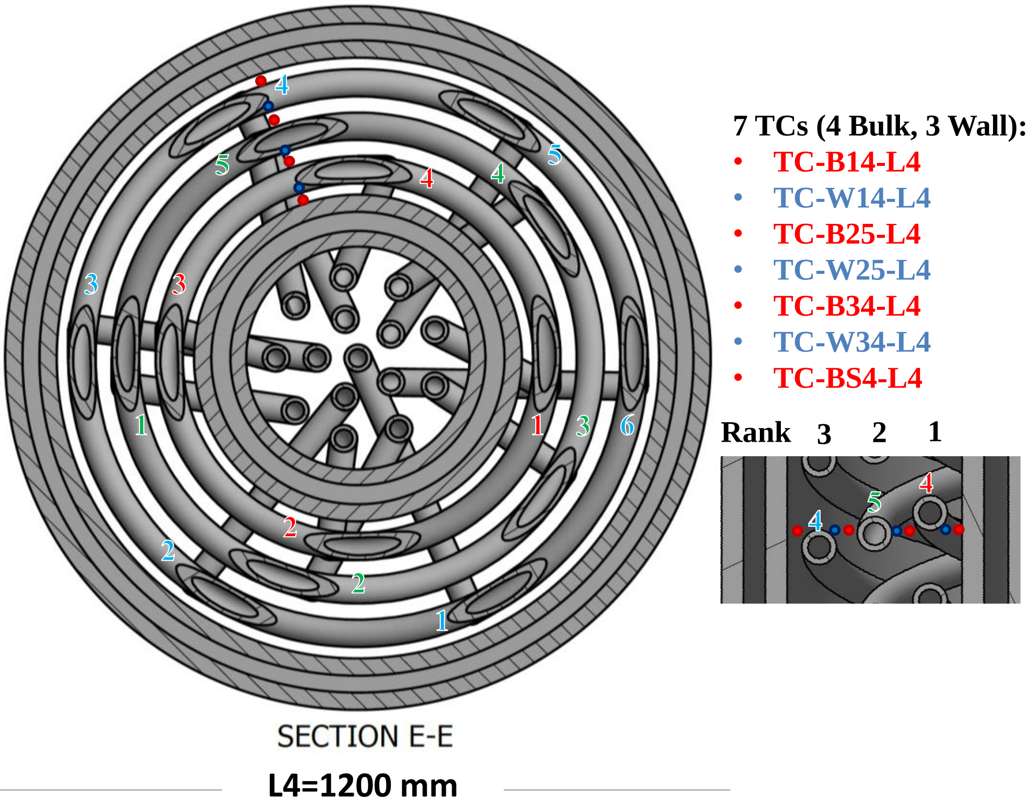

Fig. 10 – HCSG instrumentation: bulk TCs (red) and wall TCs (blue) at the Level 3

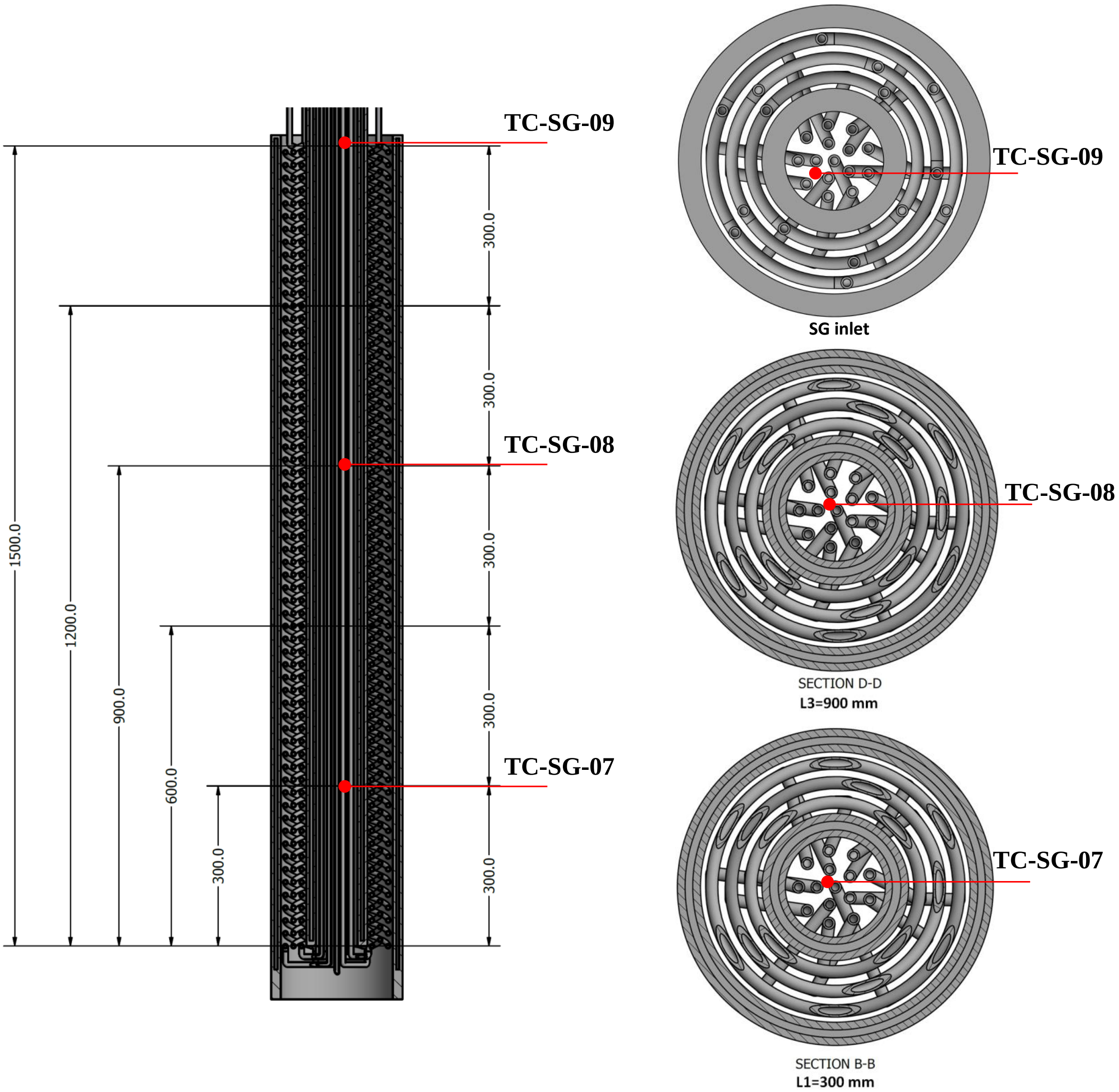

Fig. 11 – TCs positions inside the dead volume

6 RELAP5 PRELIMINARY ANALISIS

6.1 Development of the input deck

In order to estimate the number of tubes of the helical bundle, the tube length and to optimize the overall design of the SG, a numerical model has been developed using RELAP5/Mod3.3 [19], modified by ENEA with the implementation of the properties of Pb, LBE and PbLi, along with some correlations for the heat transfer for heavy liquid metals [20][21][22]: Seban-Shimazaki (used for non-bundle geometry) and Ushakov and Mikityuk (used for bundle geometries).

Fig. 8 shows the numerical 1-D model realized for the simulation. The nodalization consists of 75 hydrodynamic volumes, 73 junctions, 40 heat structures and 520 heat transfer nodes. In particular, the main components reproduced are (see Fig. 8):

- the downcomer tube bundle, simulated by the equivalent PIPE 103, consisting of 20 volumes (non-active region);
- the helical riser bundle, simulated by the equivalent PIPE 105, consisting of 30 volumes. The volumes from 105-01 to 105-20 represent the active region, while the volumes from 105-21 to 105-30 reproduce the effects of the non-active length at the SG outlet;
- the LBE pool, simulated by an equivalent channel (PIPE 203).

The time dependent volume (TMDPVOL) 101 sets the water inlet conditions in the SG and the time dependent junction (TMDPJUN) 102 works as pump providing the water mass flow rate, while TMDPVOL 107 defines the conditions at the outlet section of the SG. In the same way, TMDPVOL 201 sets the LBE inlet temperature and TMDPJUN 202 fixes the LBE mass flow rate, while the TMDPVOL 205 represents the LBE outlet.

Concerning the heat structures, the downcomer tube bundle has been assumes thermally insulated (adiabatic), since it is immersed in stagnant LBE, while a thermal connection has been simulated between the equivalent PIPE 105 (helical riser bundle) and the equivalent LBE channel, reproducing the walls of the helical tubes, considering the properties of the AISI 316L stainless steel.

As conservative assumption, the heat exchange between the tubes of the bundle and the LBE inside the separator has been neglected, such as the heat exchange between the LBE and the lower tube connections of the bundle between the downcomer tubes and riser tubes.

The analysis has been developed on the basis of the geometrical data already presented in Tab. 3 and Tab. 4, assuming the initial conditions summarized in Tab. 1 and Tab. 2.

In the following, the heat transfer correlations for LBE and water used for the RELAP5 calculations are reported. For the water side, the heat transfer correlations, depending on the flow regime, are:

- Laminar Forced Convection Model (Sellars) [10]:

$$Nu = 4.36 \quad \text{Eq 5}$$

- Turbulent Forced Convection Model (Dittus-Boelter) [10]:

$$Nu = CRe^{0.8}Pr^{n} \quad \text{Eq 6}$$

where:

- *C* is the Mc Adams coefficient (0.023);
- *n*=0.4 for heating and 0.3 for cooling;
- *Re* and *Pr* are the Reynolds number and Prandtl number, respectively.

- Nucleate Boiling Model (Chen) [10]:

$$q'' = h_{mac}(T_w - T_{spt})F + h_{mic}(T_w - T_{spt})S \quad \text{Eq 7}$$

where:

- h_{mac} is a macroscopic convection term (Dittus-Boelter equation)
- h_{mic} is a microscopic boiling term (Forster-Zuber equation)

- Transition Boiling Model (Chen) [10]:

$$q_{tb} = q_{CHF}A_f M_f + hg_g(T_w - T_g)(1 - A_f M_f) \quad \text{Eq 8}$$

- Film Boiling Model (Bromley) [10]:

$$hf_{spt} = 0.62\left[\frac{g\rho_g k_g^2(\rho_f - \rho_g)h'_{fg}C_{pg}}{L(T_w - T_{spt})Pr_g}\right]^{0.25} M_a \quad \text{Eq 9}$$

For a detailed description of all the terms of the formulas reported in Eq. 7, Eq. 8 and Eq. 9 see the dedicated sections in [10].

- CHF Model: tables and correlations reported in [10].

For the heat transfer in the helical tube bundle zone, LBE side, the Seban-Shimazaki correlation is used [11]:

$$Nu = 5 + 0.025 Pe^{0.8} \quad \text{Eq 10}$$

where Pe is the Peclet number.

Since an appropriate convective heat transfer correlation for helical tube bundle is not implemented the modified version of RELAP5, the Seban-Shimazaki correlation has been corrected with a multiplicative factor, calculated as the ratio between Seban-Shimazaki and Sherbakov correlation [12] which is used for liquid metal in helical coil bundle geometry:

$$Nu = 5.5 + 0.025\, Pe^{0.8} \quad \text{Eq 11}$$

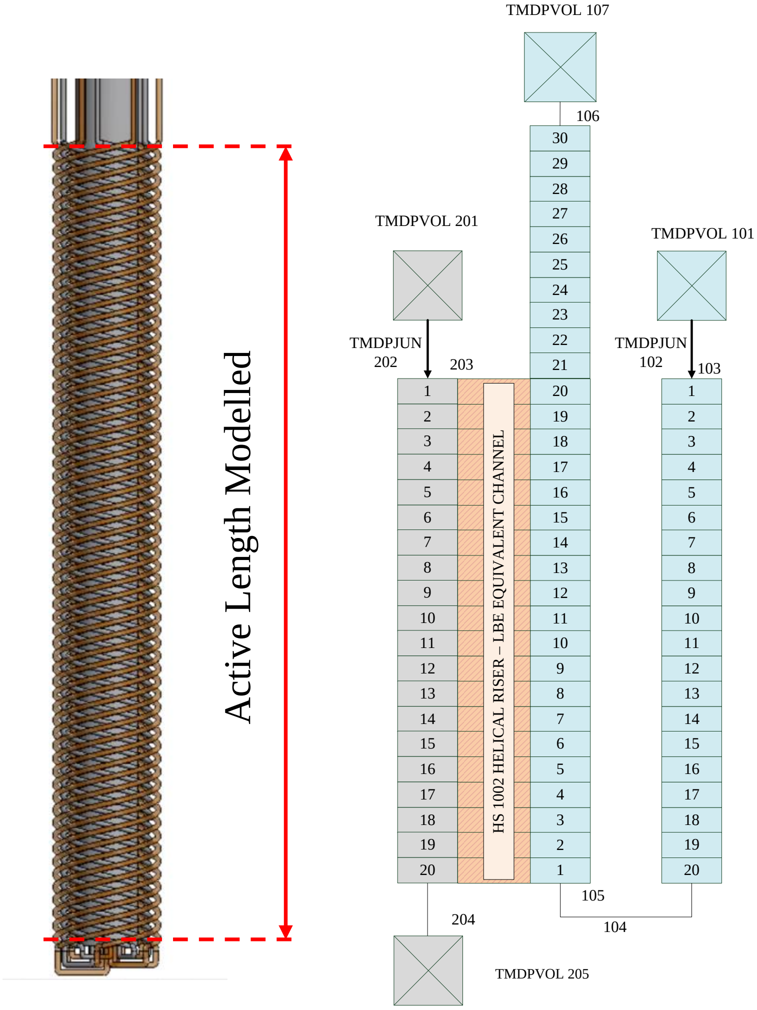

Fig. 12 – RELAP5/Mod3.3 Nodalization

6.2 RELAP5 results

On the basis of the preliminary calculations performed in Section 3, the model described above has been used to perform a series of simulations aiming at characterizing the HCSG from a thermal-hydraulic point of view in operating conditions relevant for the fission and fusion applications for which the component will be tested. In particular, three cases have been simulated, at three different secondary loop operating pressure, i.e. 9 MPa, 12 MPa and 18 MPa. The boundary conditions are summarized in Tab. 12. The water HCSG inlet temperature and mass flow rate have been set in order to be consistent with the data reported in Tab. 2. On the primary system, the LBE HCSG inlet temperature has been fixed at 480°C for all the three cases. and for each test a numerical sensitivity analysis has been executed, changing the LBE mass flow rates in three steps, i.e. 70.5, 47.0, 35.2 kg/s (reference cycle 480-400°C at 35.2 kg/s). In the following, the results of the simulations are presented in terms of LBE and H_2O flow rates, velocities, temperatures, heat transfer coefficients and power exchanged. Tab. 13, Tab. 14 and Tab. 15 summarize the main outcomes of the simulations.

Fig. 13 reports the LBE mass flow rate (set as boundary condition) and the average LBE velocities along the helical tube bundle zone. The LBE average velocities are in the range of 0.2-0.4 m/s. It can be observed that such values are consistent with the velocity range expected for the DCLL BB PbLi/water heat exchangers. In natural circulation, the LBE mass flow rate will reach lower values. This implies that the LBE velocity field is expected to be lower than 0.1 m/s, thus representative of the flow conditions of the WCLL PbLi loop and is coherent with detailed CFD numerical simulations. It must be considered that the model does not take into account the adoption of spacers which will be foreseen in order to keep the tubes in position. The presence of the spacer will slightly reduce the flow area, causing small changes in the LBE velocity field.

The power removed from the LBE by the water is reported in Fig. 14. Considering the reference case (LBE mass flow rate 35.2 kg/s), the higher fraction of power removed is achieved in the case at 9 MPa (as anticipated in Section 4) with 435 kW, while in the other cases the values are lower, i.e. 422 kW for the Case at 12 MPa and 397 kW for the case at 18 MPa. It can be observed that for reference conditions, all the cases show a power removed within the maximum range of 400-450 kW. Increasing the LBE mass flow rate, the power removed increases too for all the cases, as a consequence of the higher LBE velocity and, thus, the higher LBE heat transfer coefficient. When the mass flow rate increases at 47.0 kg/s the power removed reaches the range of 435-442kW, while it increases in a range of 445-460 kW when the mass flow rate is 70.5 kg/s.

Fig. 15, Fig. 16 and Fig. 17 report the LBE and H_2O temperatures profiles along the HCSG active length for the all the three cases and for each step of LBE mass flow rate. The inlet temperature is 480°C, then it decreases with an almost linear trend up to the outlet temperature, which assumes different values depending on the LBE mass flow rates. Considering the step with LBE mass flow rate at 35.2 kg/s (reference case, Fig. 17) a value of 394°C is obtained for the first case (9 MPa), 397°C for the second case (12 MPa) and 402°C for the third case (18 MPa). For the other steps, the outlet temperature is in range of 434-436°C (70.5 kg/s, Fig. 15) and 414-416°C (47.0 kg/s, Fig. 16). Concerning the secondary side, the water temperature along the downcomer tube remains constant for each case, since the downcomer tube bundle has been assumed thermally insulated in the numerical model. When the water enters in the riser helical tube bundle, the temperature increases rapidly up to the saturation temperature at the corresponding working pressure, proving that the vaporization starts on the bottom part of the active length. For case at 18 MPa, the saturation temperature is reached at an higher level respect to the other two cases, because of the higher sub-cooling assumed for the water inlet temperature (~22°C for the case at 18 MPa instead of 3-5°C for the other two cases). In all the cases, a high temperature steam is produced at the outlet of the helical tube bundle with a minimum value of 396.6°C reached in the case at 18 MPa and step at 35.2 kg/s (Fig. 17) and a maximum value of 463.1°C achieved in the case at 9 MPa and step at 70.5 kg/s.

A further information is given in Fig. 18 which shows the thermodynamic quality at the outlet section of the HCSG. The values are above 1.0 for all the cases, proving that the steam produced has a high degree of superheating. In addition, Fig. 19, Fig. 20 and Fig. 21 report the steam quality along the helical tube bundle. It can be observed that the steam quality increases with an almost linear trend, reaching a value of 1.0 at the HCSG outlet section in all the cases.

Fig. 22, Fig. 23 and Fig. 24 show the LBE convective Heat Transfer Coefficient (HTC) along the helical tube bundle zone for all the cases. It can be observed that the values are similar among the cases, since the LBE flow conditions (i.e. mass flow rate and velocity) are the same. The higher value (avg. 5070 W/(m^2*K)) is reached when the LBE mass flow rate is 70.5 kg/s, then it reduces at 4170 W/(m^2*K) and 3680 W/(m^2*K) when the LBE mass flow rate is 47.0 kg/s and 35.2 kg/s, respectively. Finally, the water heat transfer coefficient is reported in Fig. 25, Fig. 26 and Fig. 27. Since the vaporization occurs at the beginning of the active length, the HTC assumes the higher values at the bottom of the helical tube bundle. In case at 9 MPa the HTC reaches the maximum value 65750 W/(m^2*K), in case at 12 MPa it is 70210 W/(m^2*K)) and in case at 18 MPa it is 83843 W/(m^2*K)). It can be noted that in the case at 18 MPa the maximum HTC is reached at an higher height, since the feedwater has an higher degree of sub-cooling respect to the other two cases. The thermal crisis occurs in a height range of 0.2-0.6 m. After that, the HTC suddenly decreases up to the final value of ~3000 W/(m^2*K) in the case at 9 MPa, ~4000 W/(m^2*K) in the case at 12 MPa and ~6000 W/(m^2*K) in the case at 18 MPa.

Parameter	Unit	Case @9 MPa	Case @12 MPa	Case @18 MPa
LBE mass flow rate	[kg/s]	70.5 47.0 35.2	70.5 47.0 35.2	70.5 47.0 35.2
HCSG T inlet LBE	[°C]	480	480	480
H2O mass flow rate	[kg/s]	0.23	0.25	0.3
P H2O	[MPa]	9	12	18
HCSG T inlet H2O	[°C]	300	320	335

Tab. 12 – RELAP5 primary and secondary system boundary conditions

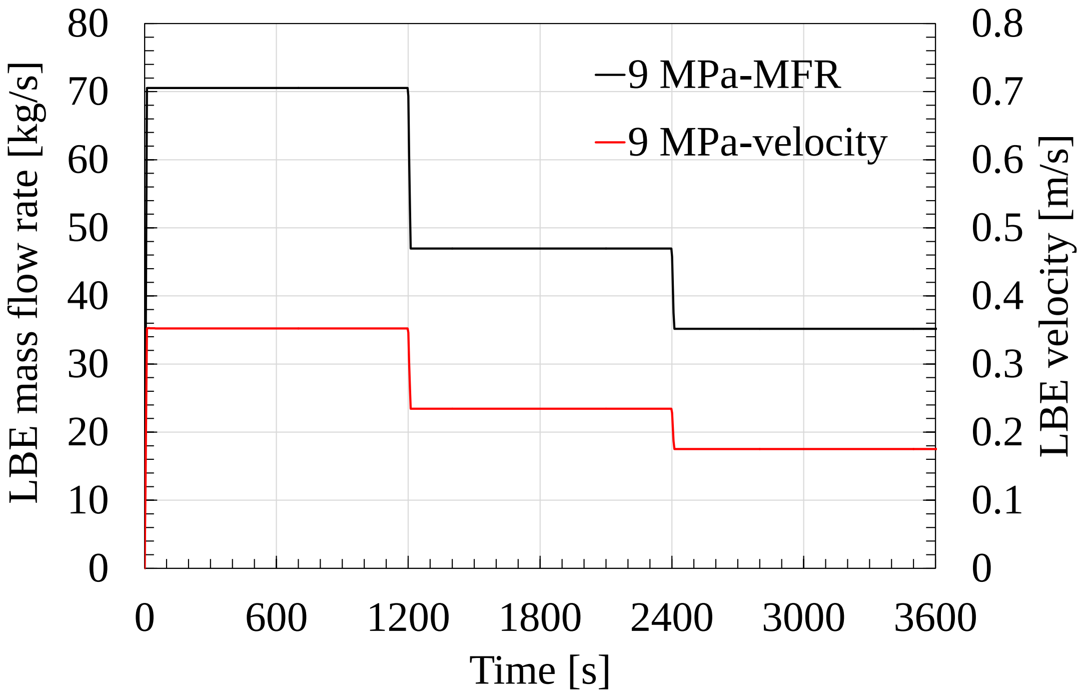

Fig. 13 – LBE mass flow rate and velocity along the helical tube bundle zone during Case @9 MPa

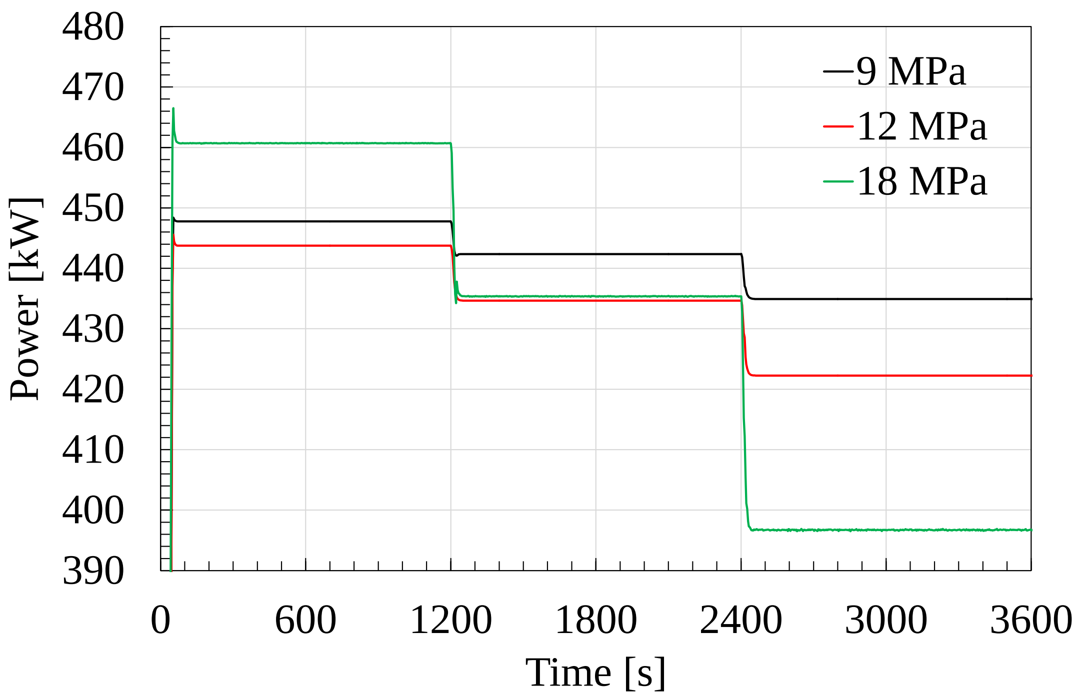

Fig. 14 – Power removed during the cases studied

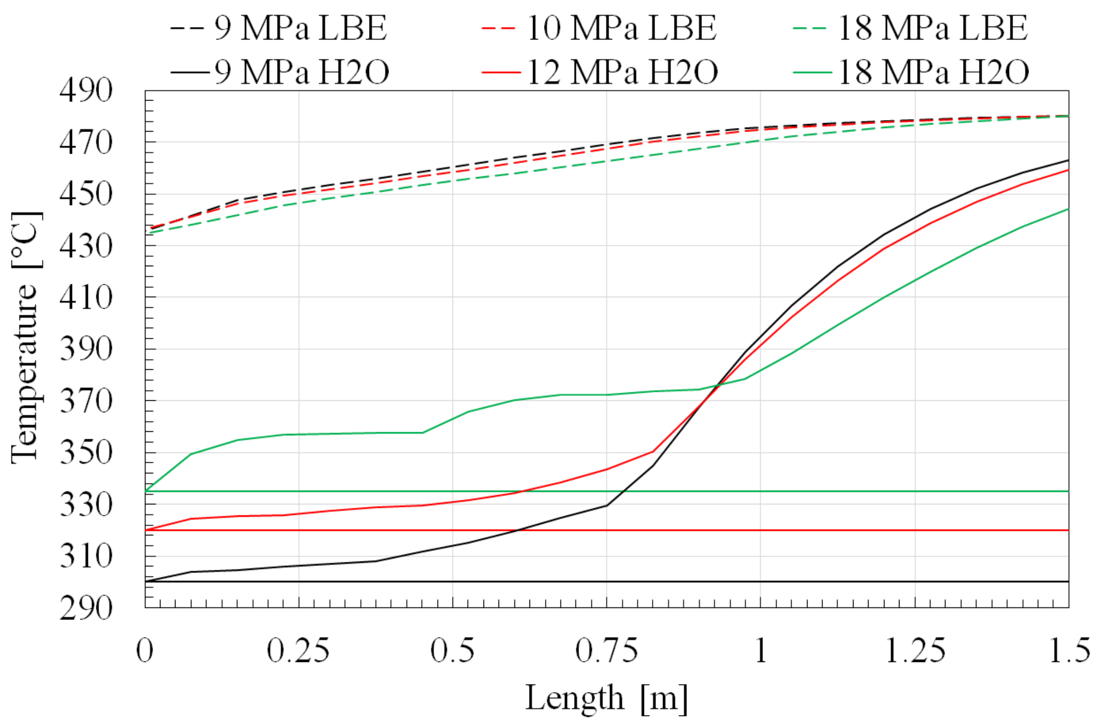

Fig. 15 – LBE and H2O temperatures along the active length during the step at 70.5 kg/s

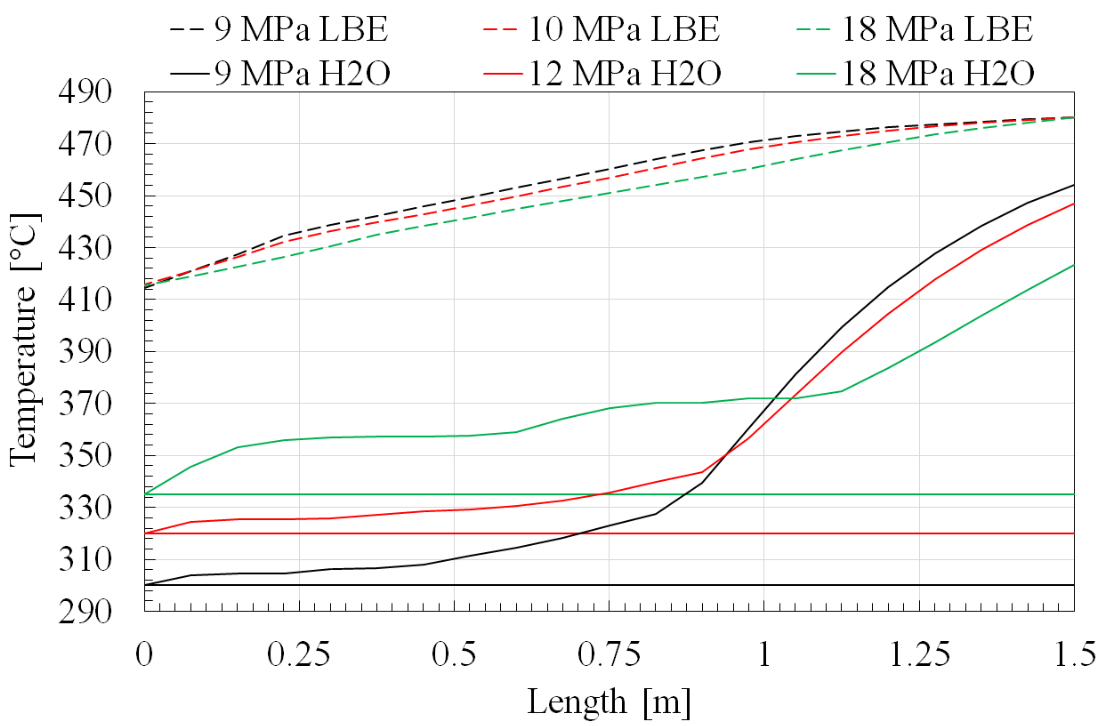

Fig. 16 – LBE and H2O temperatures along the active length during the step at 47.0 kg/s

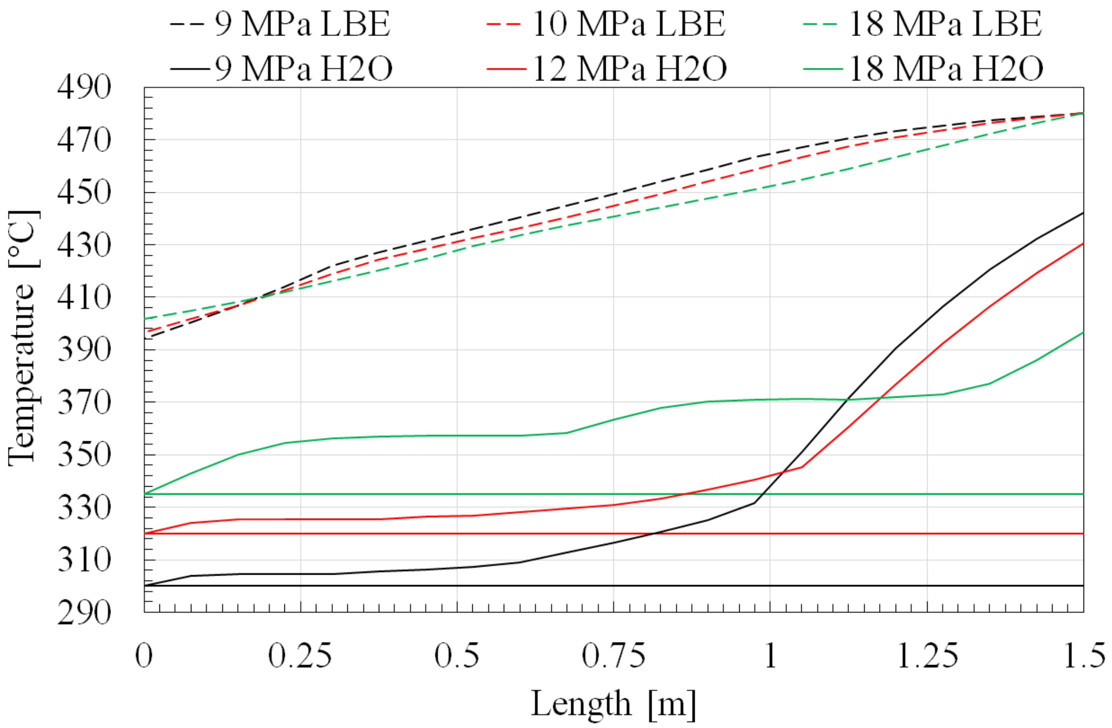

Fig. 17 – LBE and H2O temperatures along the active length during the step at 35.2 kg/s

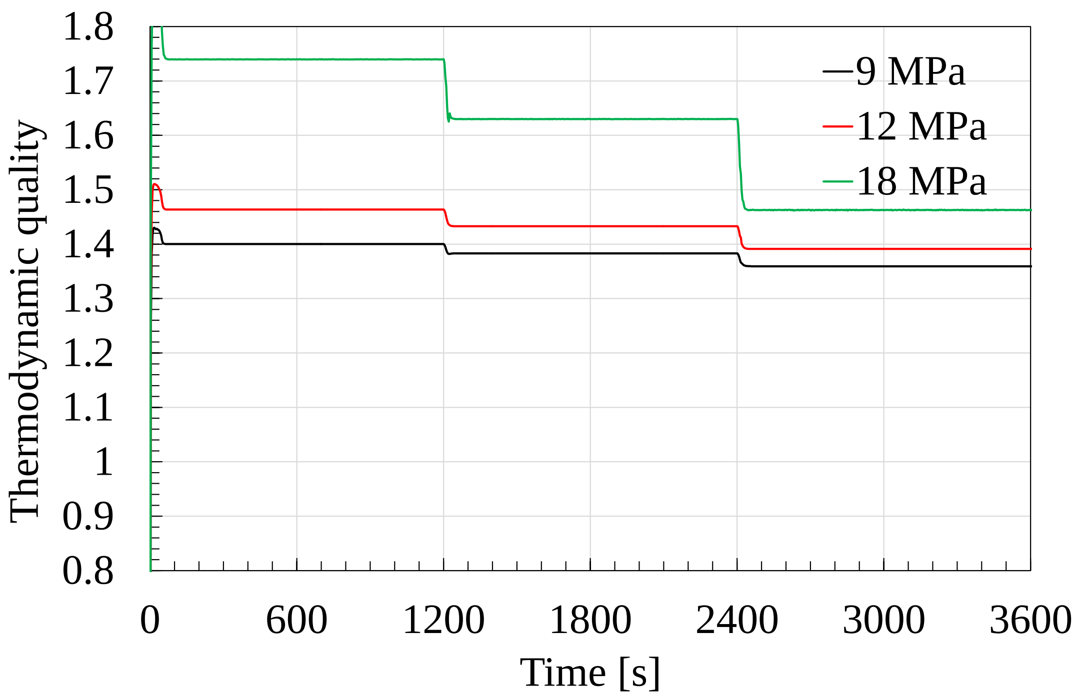

Fig. 18 – Thermodynamic quality achieved at the HCSG outlet section during the cases studied

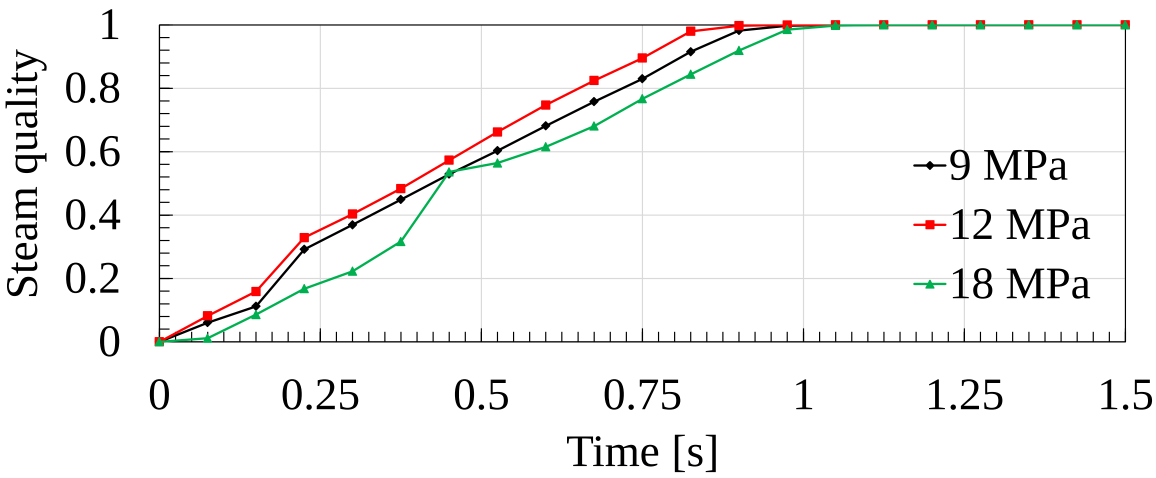

Fig. 19 – Steam quality along the active length during the step at 70.5 kg/s

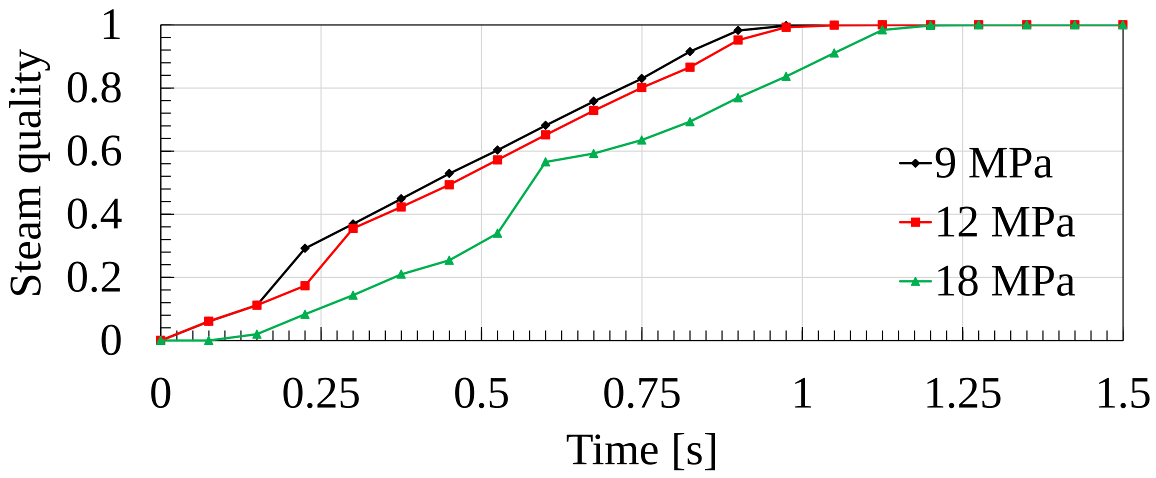

Fig. 20 – Steam quality along the active length during the step at 47.0 kg/s

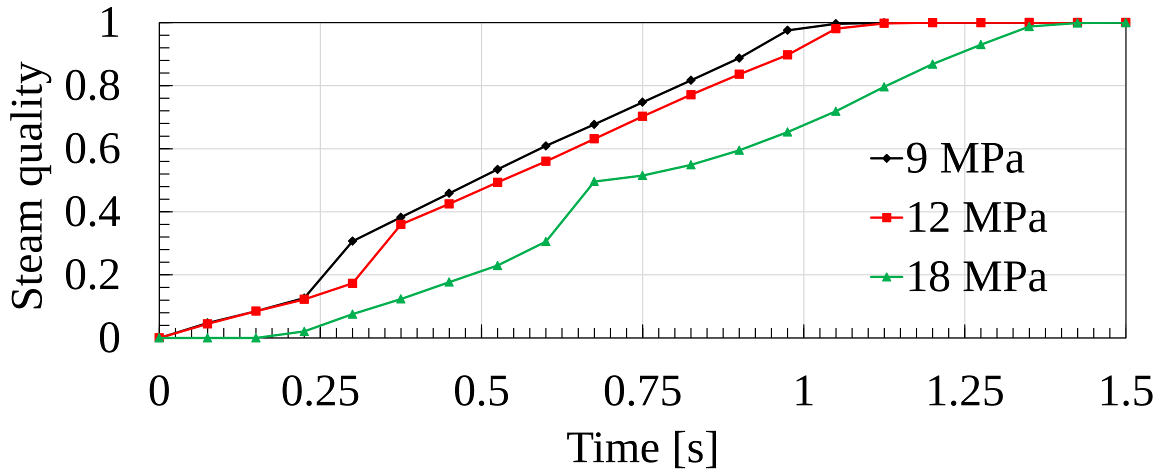

Fig. 21 – Steam quality along the active length during the step at 35.2 kg/s

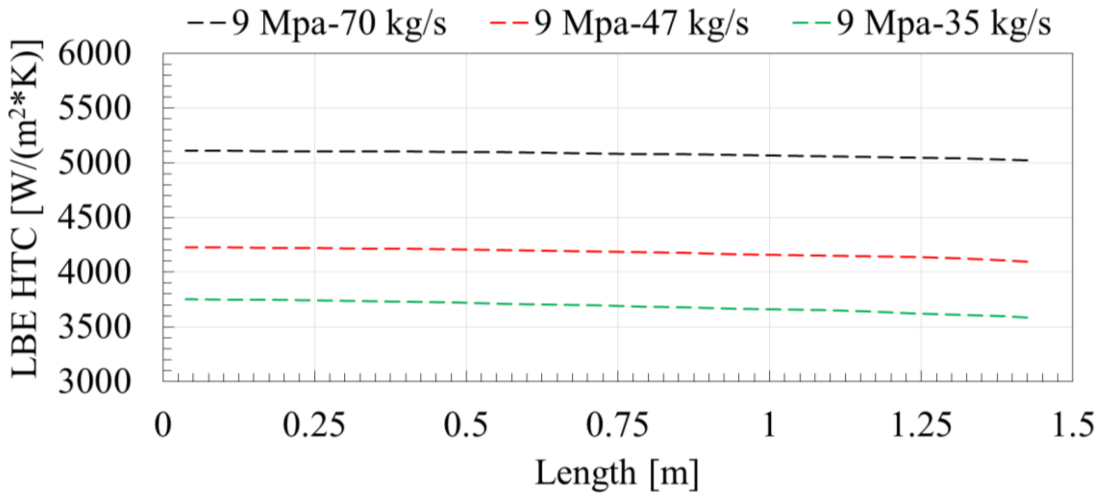

Fig. 22 – Case @9 MPa, LBE heat transfer coefficient in the helical tube bundle zone

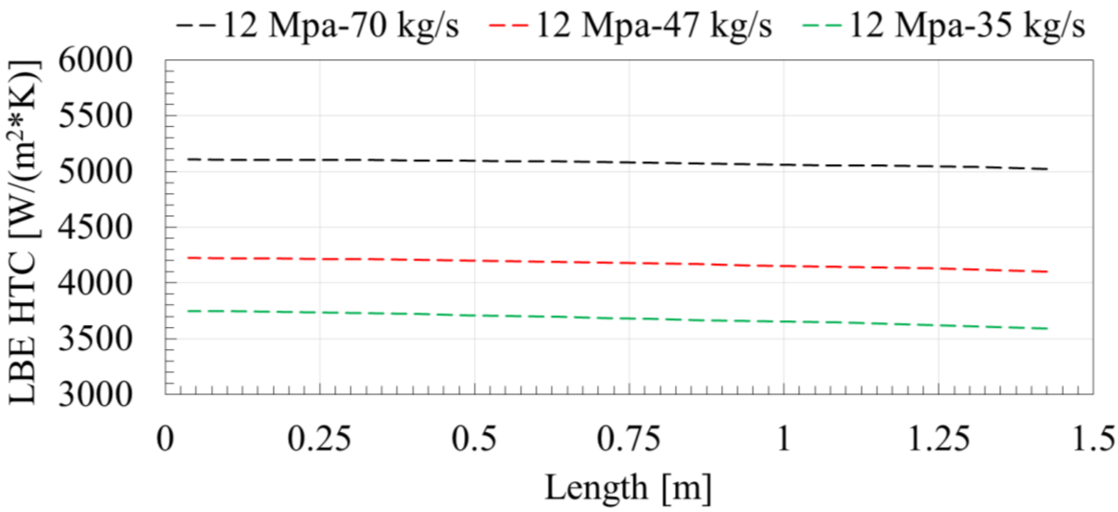

Fig. 23 – Case @12 MPa, LBE heat transfer coefficient in the helical tube bundle zone

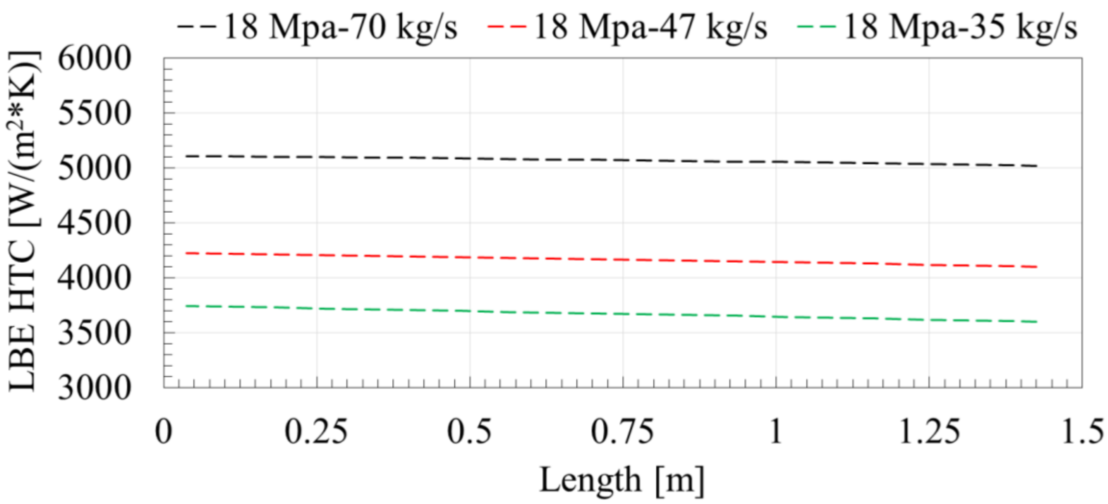

Fig. 24 – Case @18 MPa, LBE heat transfer coefficient in the helical tube bundle zone

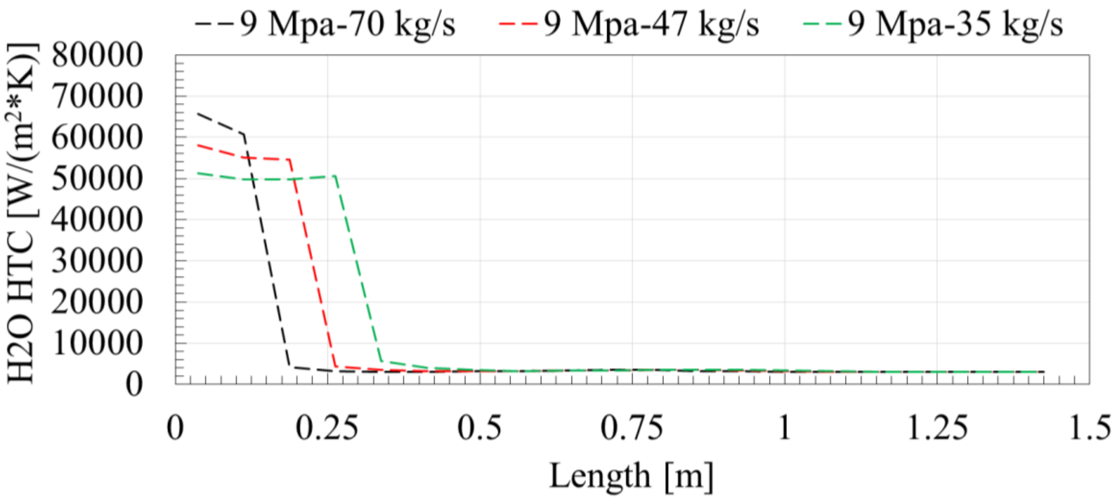

Fig. 25 – Case @9 MPa, H2O heat transfer coefficient in the helical tube bundle zone

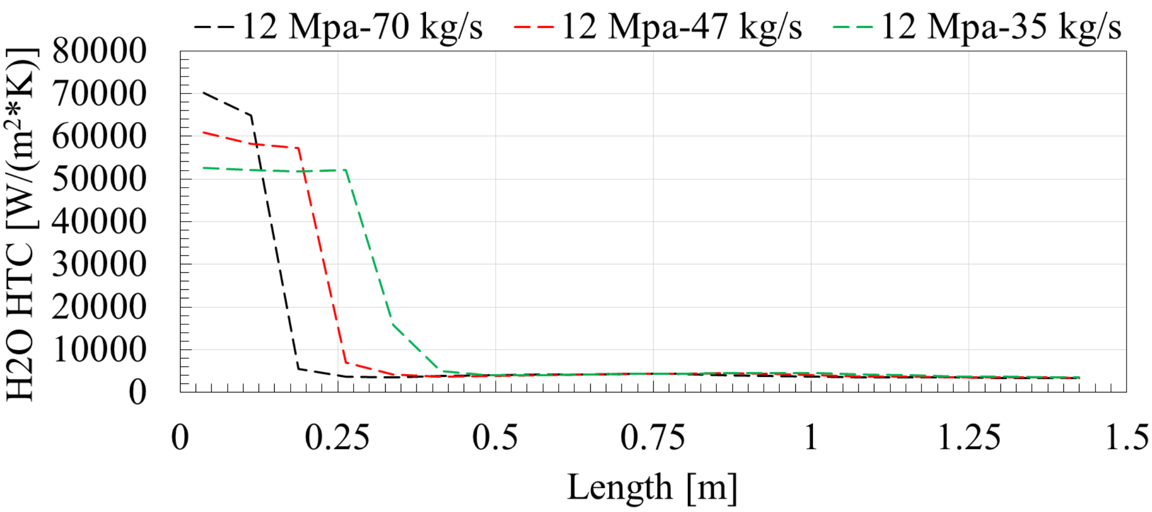

Fig. 26 – Case @12 MPa, H2O heat transfer coefficient in the helical tube bundle zone

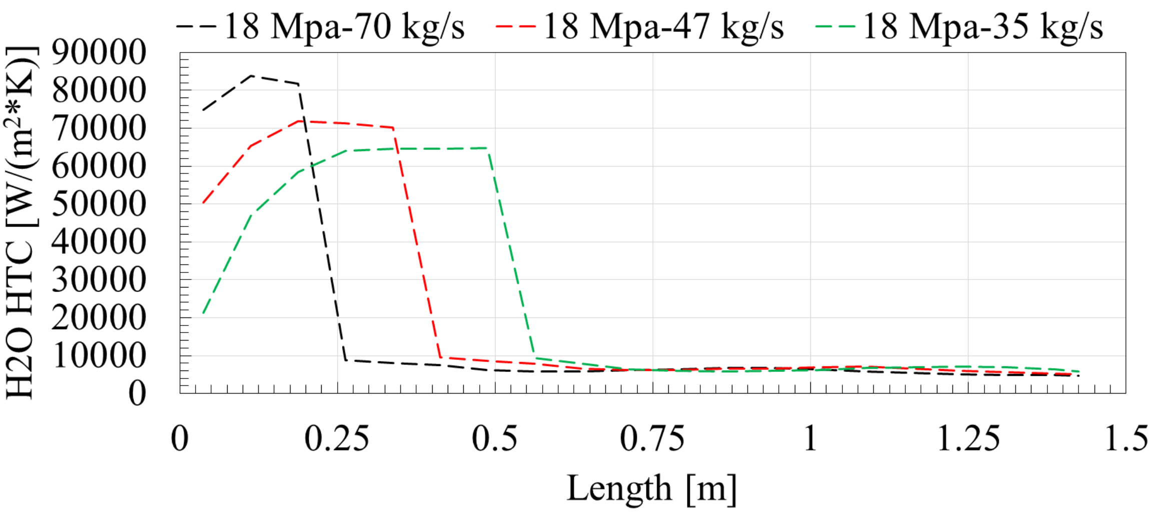

Fig. 27 – Case @18 MPa, H2O heat transfer coefficient in the helical tube bundle zone

Parameter	Unit	Step 70.5 kg/s	Step 47.0 kg/s	Step 35.2 kg/s
LBE velocity	[m/s]	0.35	0.24	0.18
Power removed	[kW]	448	442	435
HCSG T out LBE	[°C]	435.8	414.5	394.2
HCSG T out H2O	[°C]	463.1	454.2	442.1
Steam quality outlet	----	1.0	1.0	1.0
Thermodynamic quality	----	1.40	1.38	1.36
Steam velocity outlet	[m/s]	17.2	16.9	16.5
HTC LBE	[W/(m^2*K)]	5077	4178	3684
HTC H2O (max vap.)	[W/(m^2*K)]	65750	58037	51205
HTC H2O (avg. steam)	[W/(m^2*K)]	3130	3168	3248

Tab. 13 – Summary of the RELAP5 main outcomes during case at 9 MPa

Parameter	Unit	Step 70.5 kg/s	Step 47.0 kg/s	Step 35.2 kg/s
LBE velocity	[m/s]	0.35	0.24	0.18
Power removed	[kW]	444	435	422
HCSG T out LBE	[°C]	436.2	415.6	396.6
HCSG T out H2O	[°C]	459.2	446.8	430.4
Steam quality outlet	----	1.0	1.0	1.0
Thermodynamic quality	----	1.46	1.43	1.39
Steam velocity outlet	[m/s]	13.4	13.1	12.5
HTC LBE	[W/(m^2*K)]	5075	4174	3679
HTC H2O (max vap.)	[W/(m^2*K)]	70210	60857	52563
HTC H2O (avg. steam)	[W/(m^2*K)]	3794	3917	4033

Tab. 14 – Summary of the RELAP5 main outcomes during case at 12 MPa

Parameter	Unit	Step 70.5 kg/s	Step 47.0 kg/s	Step 35.2 kg/s
LBE velocity	[m/s]	0.35	0.24	0.18
Power removed	[kW]	461	435	397
HCSG T out LBE	[°C]	434.5	415.5	401.7
HCSG T out H2O	[°C]	444.3	423.3	396.6
Steam quality outlet	----	1.0	1.0	1.0
Thermodynamic quality	----	1.74	1.63	1.46
Steam velocity outlet	[m/s]	9.4	8.7	7.6
HTC LBE	[W/(m^2*K)]	5068	4165	3672
HTC H2O (max vap.)	[W/(m^2*K)]	83843	71843	64575
HTC H2O (avg. steam)	[W/(m^2*K)]	5740	6187	6384

Tab. 15 – Summary of the RELAP5 main outcomes during case at 18 MPa

7 CFD PRELIMINARY ANALISIS

A preliminary CFD analysis has been carried out on the LBE shell side of the HCSG to assess fluid flow and pressure losses in the component. These figures are important to characterize the behaviour of the HCSG and to design the height of the separator. The analysis considers the nominal flow rate of 35.17 kg/s. For the modelling and mesh, the exact geometry of the HCSG has been reproduced in the basis of the data reported in Tab. 3 and Tab. 4 and an unstructured mesh with inflation layer at the tube and shell walls has been built. The adopted inflation guarantees y^+=1 at the walls in nominal conditions and therefore the flow viscous sublayer and boundary layer was described explicitly without the use of wall functions or other approximations. The total number of nodes and elements was respectively 17 million and 48 million. The turbulence model adopted was the SST k-omega and full convergence was achieved in the calculation with residuals at 10^{-5}-10^{-6}. The simulation required 1 day in a 24 Xeon parallel computer.

Fig. 28 shows the streamwise velocity distribution in the middle cross section of the HCSG. The maximum LBE velocity is about 0.3-0.4 m/s and is reached in a peripherals channels close to the tubes. A weak streamwise recirculation with positive velocities is evidenced in the intermediate rank. The average velocity in the section is about 0.18 m/s and is coherent with the RELAP5 analysis.

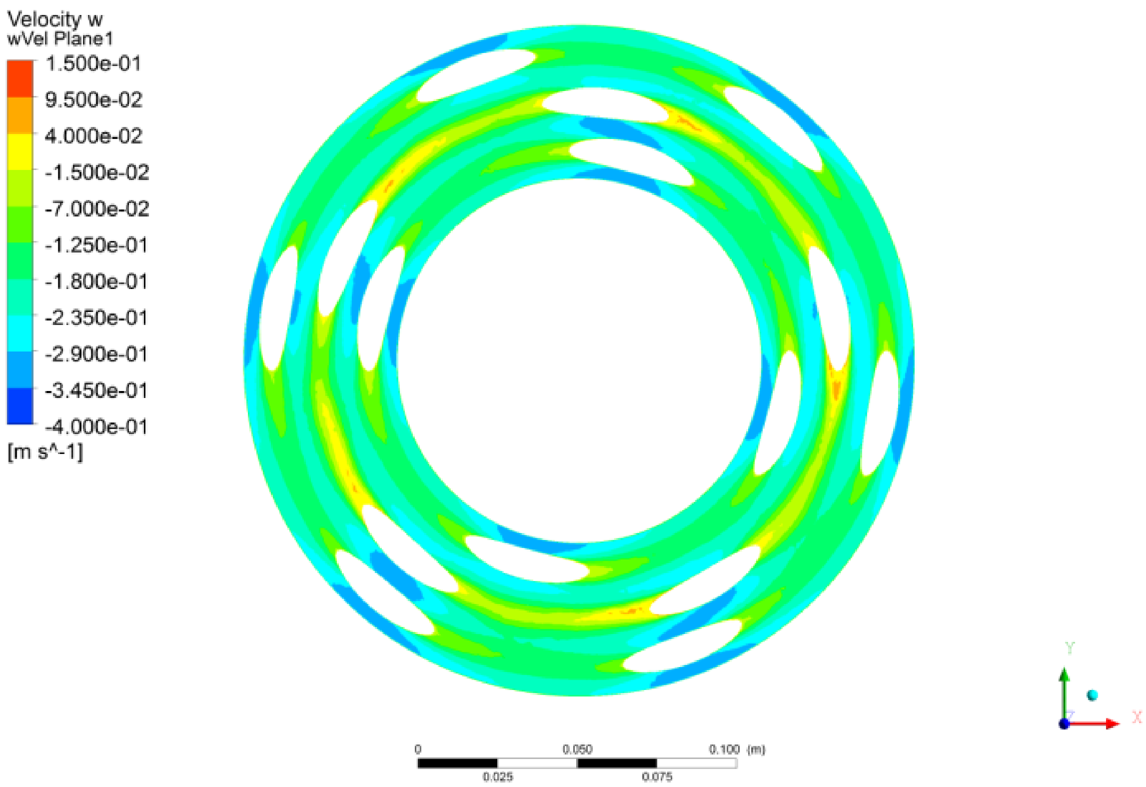

Fig. 28 – Streamwise velocity distribution in a cross section in the middle of HCSG

Fig. 29 shows the 3D streamlines in the domain. It can be noticed that the streamlines are not straight but have a helicoidal clockwise shape due to the fact that the pipes are helicoidally wrapped and two ranks have a clockwise direction which is dominant. Due to this feature, a strong secondary circulation is present and this will enhance heat transfer and increase pressure drop. This is shown in Fig. 30 were the secondary flow in the middle cross section is represented. The circulation is clockwise (seen from the top) and it is particularly strong in the inner and in the outer ranks with a secondary velocity around 0.2 m/s, therefore of the same order of the streamwise main component. Finally, the computed pressure drop across the component is about 13 kPa (0.13 bar). This is the reference value to dimension the height of the separator in the THETIS TS.

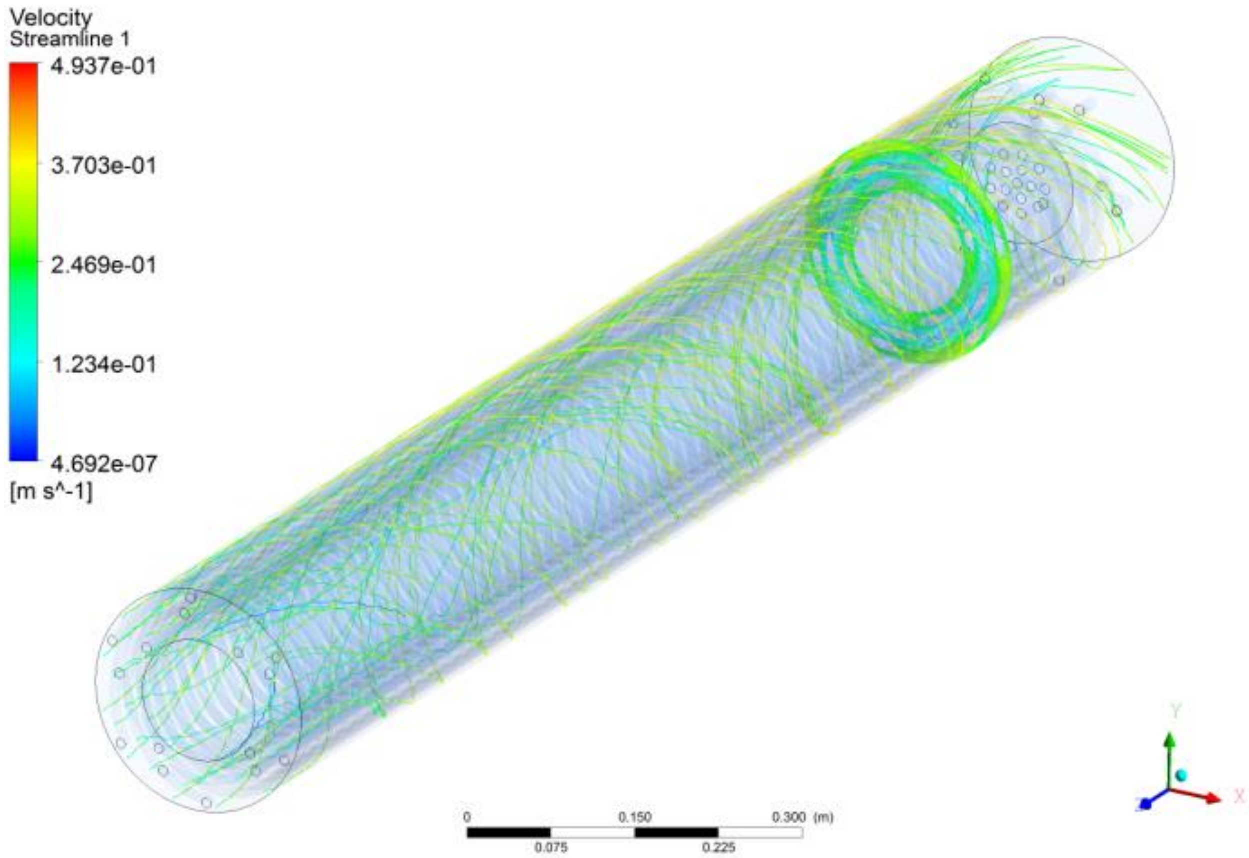

Fig. 29 – 3D streamline in the HCSG domain

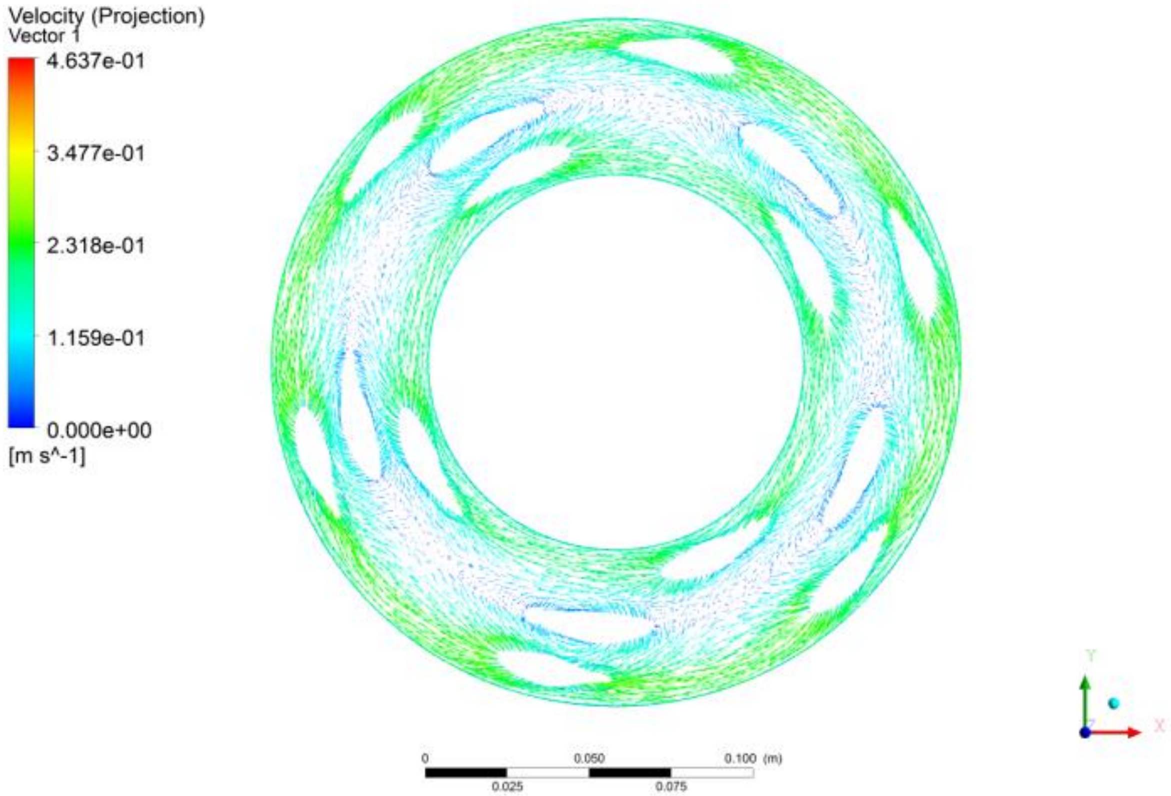

Fig. 30 – Secondary flow in the middle cross-section of the HCSG domain LBE side

8 CONCLUSIONS

The present document describes the preliminary design of the new HCSG mock-up for the THETIS test section. The main information about the geometrical features and the instrumentation installed are reported. The overall design of the HCSG has been optimized by means of numerical simulations performed with the thermal-hydraulic system code RELAP5/Mod3.3, modified by ENEA with the implementation of the properties of Pb, LBE and PbLi, along with some correlations for the heat transfer for heavy liquid metals.

The final layout of the HCSG consists of by a helical tube bundle having a height of 1.5 m, surrounded by a double wall shell of 1.62 m height. A total of 15 helical tubes are arranged in three horizontal ranks: the inner rank is composed of 4 tubes, the intermediate one is composed of 5 tubes and the outer rank has 6 tubes. An overall number of 41 TCs (hot junction isolated, N-type) is implemented in the LBE side of the HCSG for a complete thermal-hydraulic characterization of the component. Additional TCs are foreseen on the secondary side to measure the inlet and outlet water temperature. A differential pressure transmitter is foreseen to acquire the pressure drops across the feedwater manifold and steam chamber.

A preliminary analysis to assess the main operative parameters of the facility showed that in order to be within the maximum power 1 MW available for the CIRCE facility, the thermal duty of the HCSG has to be in the range of 400-450 kW. Assuming a power of 400 kW and a reference LBE thermal cycle with a HCSG inlet-outlet temperature of 480-400°C, the LBE mass flow rate needed is 35.2 kg/s, which is within the operating range of the MCP. Furthermore, three water thermal cycles have been considered for the secondary loop, characterized by three working pressures, i.e. 9 MPa, 12 MPa and 18 MPa and three feedwater temperatures, i.e. 300°C (case at 9 MPa), 320°C (case at 12 MPa) and 335°C (case at 18 MPa). The water mass flow rates calculated are in the range of 0.23-0.3 kg/s, which are consistent with the mass flow rates elaborated by the secondary water pump.

On the basis of the preliminary calculations performed, the RELAP5 model has been used to perform a series of simulations aiming at characterizing the HCSG from a thermal-hydraulic point of view in operating conditions relevant for the fission and fusion applications. Three cases have been simulated, at three different secondary loop operating pressure and temperatures specified above. On the primary system, the LBE HCSG inlet temperature has been fixed at 480°C for all the three cases, and for each test a numerical sensitivity analysis has been executed, changing the LBE mass flow rates in three steps, i.e. 70.5, 47.0, 35.2 kg/s. The simulation showed that in all the cases the power removed by the HCSG is within or very close to the range of 400-450 kW and high temperature steam is produced in a range of 400-460°C, proving that the component is suitable for the fission and fusion applications for which it is designed.

A CFD hydrodynamic analysis on the LBE shell side has been carried out to evidence flow features and compute the pressure drop in nominal conditions (mass flow rate 35.2 kg/s). Results showed the presence of a strong helical wrapped circulation determined by the geometry of the three ranks of tubes. The secondary circulation is of the same order of the main streamwise circulation with velocities around 0.2 m/s and it is expected that it could enhance heat transfer. The pressure drop in the HCSG has been computed as 13 kPa (0.13 bar).

REFERENCES

[1] A. Pesetti, N. Forgione, V. Narcisi, P. Lorusso, F. Giannetti, M. Tarantino, A. Del Nevo ENEA CIRCE-HERO Test Facility: Geometry And Instrumentation Description CI-I-R-343, ENEA report, June, 22, 2018.

[2] M. Tarantino, PRIMARY PUMP per impianto sperimentale a metallo liquido pesante CIRCE, CI-D-S-355, ENEA report, October, 11, 2018.

[3] P. Lorusso, D. Martelli, I. Di Piazza, A. Del Nevo, M. Tarantino, Preliminary requirements of HCSG test section for CIRCE facility, CI-I-R-449, ENEA report, March, 24, 2020.

[4] Lorusso, P., et al., Protected loss of flow accident simulation in CIRCE-HERO facility: experimental test and system code assessment, Ibaraki, Proc. 27th Int. Conf. Nucl. Eng, (ICONE 2019), 19-24 2019 May.

[5] Lorusso, P., et al., Experimental Analysis Of Stationary And Transient Scenarios Of ALFRED Steam Generator Bayonet Tube In CIRCE-HERO Facility, Nuclear Engineering and Design 352 (2019) 110169, https://doi.org/10.1016/j.nucengdes.2019.110169.

[6] OECD/NEA Nuclear Science Committee, Handbook on Lead-bismuth Eutectic Alloy and Lead Properties, Materials Compatibility, edition, Thermal-hydraulics and Technologies, 2015.

[7] Water TH properties, http://www.peacesoftware.de/einigewerte/wasser_dampf_e.html.

[8] Lorusso, P., et al., PbLi Heat Exchanger and fluid technology - As built PbLi/H2O HX test facility report, EUROfusion Internal Deliverable BOP-4.1.1-T002, Sept. 2019.

[9] P. Lorusso, I. Di Piazza, D. Martelli, A. Musolesi, A. Del Nevo, M. Tarantino, Primary loop instrumentation of the THETIS test section for the CIRCE facility, CI-I-R-517, ENEA report, October, 21, 2020.

[10] The RELAP5 Code Development Team, "RELAP5/MOD3 Code Manual Volume IV: Models And Correlations", INEL-95/0174.

[11] Seban R.A., Shimazaki T.T., "Heat transfer to a fluid flowing turbulently in a smooth pipe with walls at constant temperature", Transactions of the ASME, Vol. 73, pp. 803-809, 1951.

[12] Beznosov, A. V., et al. Experimental Studies of Heat Transfer Characteristics and Properties of the Cross-Flow Pipe Flow Melt Lead. Open Journal of Microphysics, 2014, 4, 54-65. DOI. 10.4236/ojm.2014.44008.

DISTRIBUTION LIST

#	NOME	ISTITUZIONE	E-MAIL
1	A. Del Nevo	*ENEA*	alessandro.delnevo@enea.it
2	I. Di Piazza	*ENEA*	ivan.dipiazza@enea.it
5	P. Lorusso	*ENEA*	pierdomenico.lorusso@enea.it
3	D. Martelli	*ENEA*	daniele.martelli@enea.it
6	A. Musolesi	*ENEA*	andrea.musolesi@enea.it
4	M. Tarantino	*ENEA*	mariano.tarantino@enea.it
	ARCHIVIO	*ENEA*	

APPENDIX 1

Technical drawing of the HCSG

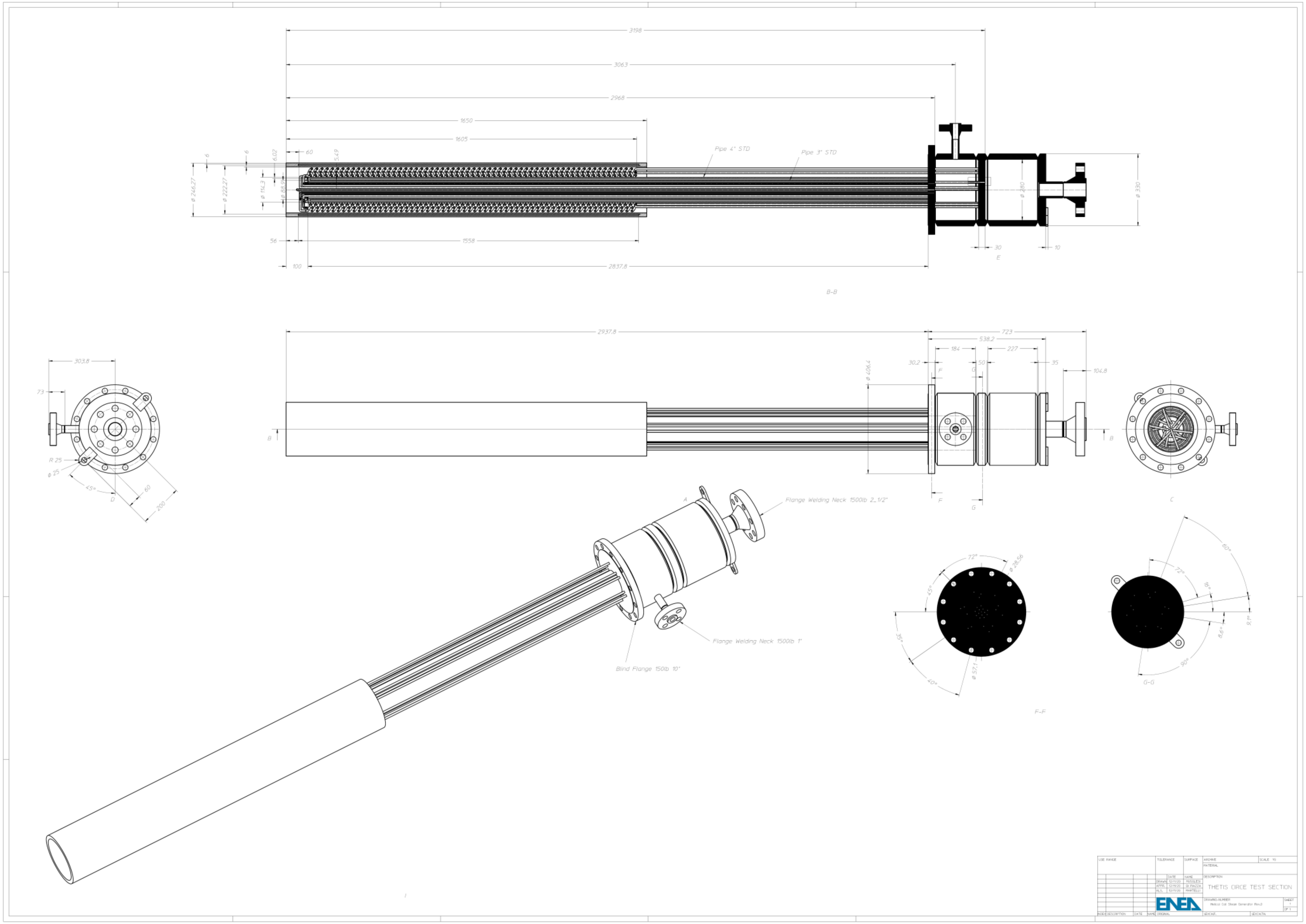

B-B
Pipe 4" STD
Pipe 3" STD
F-F
G-G
Flange Welding Neck 1500lb 2_1/2"
Flange Welding Neck 1500lb 1"
Blind Flange 150lb 10"
USE RANGE
TOLERANCE
SURFACE
ARCHIVE
SCALE 1:5
MATERIAL
DATE
NAME
DRAWN 12/11/20 MUSOLESI
APPR. 12/11/20 DI PIAZZA
RLS. 12/11/20 MARTELLI
DESCRIPTION
THETIS CIRCE TEST SECTION
DRAWING-NUMBER
Helical Coil Steam Generator Rev.2
SHEET 1
OF 1
INDEX DESCRIPTION DATE NAME ORIGINAL